R. & M. No. 3427

LIBRARY ROYAL AIRCRAFT ESTABLISHMENT BEDFORD.

MINISTRY OF AVIATION

AERONAUTICAL RESEARCH COUNCIL
REPORTS AND MEMORANDA

Experiments on Two-Dimensional Base Flow at Subsonic and Transonic Speeds

By J. F. NASH, V. G. QUINCEY and J. CALLINAN

LONDON: HER MAJESTY'S STATIONERY OFFICE
1966
PRICE £1 11s. 6d. NET

Experiments on Two-Dimensional Base Flow at Subsonic and Transonic Speeds

By J. F. NASH, V. G. QUINCEY and J. CALLINAN

*Reports and Memoranda No. 3427**
January, 1963

Summary.

A report is presented of a series of experiments aimed at an investigation of the fundamental mechanisms of the flow behind an isolated blunt-trailing-edge section, and a rearward-facing step, at subsonic and transonic speeds.

Pressure measurements and flow photography formed the principal research tools, but in connection with the tests on the isolated section an extensive wake exploration and a study of the vortex-shedding process were carried out. Tests were also made of simple devices which interfere with the formation of the vortex street. These tests are useful both from a basic research aspect and insofar as they indicate possible methods of reducing base drag.

A careful study is made of the events which are associated with the transition, at transonic speeds, from the subsonic vortex-street régime to the supersonic steady-flow régime.

The tests on the step were aimed chiefly at providing information on the non-periodic base flow which would exist behind a blunt-trailing-edge aerofoil section at subsonic and transonic speeds if the formation of the vortex street could be inhibited.

LIST OF CONTENTS

Section

1. Introduction
2. Experimental Details
3. Tests on a Blunt-Trailing-Edge Section
4. The Flow Past a Step
5. The Effect of a Splitter Plate on the Flow Past an Isolated Section
6. Results for other Base Configurations
7. Concluding Remarks

Acknowledgement

Notation

References

Illustrations—Figs. 1 to 48

Detachable Abstract Cards

* Replaces N.P.L. Aero. Report No. 1070—A.R.C. 25 070.
Published with the permission of the Director, National Physical Laboratory.

1. *Introduction*

1.1. For a number of years there has been an interest in the use of blunt-trailing-edge wings for supersonic aircraft. It was pointed out at an early stage[1,2] that the design of a wing section with a rearward position of maximum thickness and a blunt trailing edge could make possible a reduction of the surface slopes over the forebody and an associated decrease in the section wave drag. Moreover in certain cases the decrease in wave drag was more than enough to offset the drag penalty incurred due to the low pressure on the base. The structural advantages of wings of this type were, of course, a further attraction. A large research effort has been directed to the investigation of two-dimensional base flows at supersonic speeds (*see* Ref. 3, e.g.) with a view to the prediction of the base pressure, and theories have been proposed although several of these have since been shown to require important modifications.

On the other hand relatively little attention has been paid to the base-pressure characteristics in the off-design subsonic and transonic flight phases. Of the few exceptions, measurements of base pressure at transonic speeds on one aircraft configuration[4] have yielded data which are unrepresentative and which would in many cases be optimistic if used to predict the base drag of other configurations. The lack of reliable information at transonic speeds would appear to be a serious omission since the base drag on both two-dimensional[3] and slender wings[5] is then generally high, and might adversely affect the performance of an aircraft designed for cruise at supersonic speeds.

The need for information on base flows at subsonic and transonic speeds is further emphasised by the interest which has recently been aroused in the possibility of using blunt-trailing-edge wings for flight at high subsonic speeds, or at supersonic speeds if the angle of sweep is sufficient to maintain a subsonic-type flow normal to the leading edge[6,7]. Whereas at supersonic speeds the acceptance of a blunt trailing edge can be seen to bring about a reduction of the wave drag, a subsonic-type aerofoil section is usually designed to be free from wave drag at the cruise condition. Furthermore at subsonic speeds not only does the use of a blunt trailing edge incur a 'base drag' since the base pressure is normally lower than free-stream static pressure, but the pressure recovery over the rear of the aerofoil is to some extent lost. Nevertheless, aside from the structural attractions, it has been possible to show that at high subsonic speeds the reduction in surface slopes can be exploited to achieve a higher drag-rise Mach number and a delay in the onset of separation effects[7,8]. Also, by the use of lower-surface rear camber[9], it is easier to realise a substantially uniform chordwise loading than on a conventional aerofoil.

Although the potential advantages of blunt-trailing-edge wings at subsonic speeds are real and significant the successful application of the principles would appear to depend on the achievement of reasonably low values of the base drag.

1.2. At supersonic speeds a base-flow model can be constructed which considers nothing more than steady-flow components, and on this basis realistic base-pressure data can be predicted for a range of conditions. It can be shown[10] that at a given Mach number the base pressure rises with increase of the ratio of the boundary-layer momentum thickness ahead of the base, to the base height. In the subsonic case, on the other hand, it has been noted[3] that two-dimensional base flows are frequently periodic in character, involving the formation of a vortex street. The classical 'bluff-cylinder' problem in low-speed flow is an example of this, although the preoccupation of certain writers with this particular example has led to some confusion as to whether the periodic phenomena are confined to low Reynolds numbers. In the case of a circular cylinder the vortex shedding is most easily observed below the critical Reynolds number when the separation points are on the windward side of the cylinder. Above the critical Reynolds number the separation points more rearwards (leading to a narrower wake) and it has been reported (Ref. 11, e.g.) that the vortex street gives way to a more-or-less random turbulent wake. The more recent work of Roshko (Ref. 12) and others has now demonstrated the persistence of periodic effects at Reynolds numbers well above the critical. In the light of this it seems clear that vortex shedding is a feature of the flow past circular cylinders throughout the Reynolds number range but that the vortices were not detected in the earlier investigations because they are more difficult to see.

The same confusion has not arisen in the study of the flow past other body shapes and in these fields, in particular, vortex streets in turbulent flow have been accepted for many years (*see*, for example, Refs. 13, 14).

Attempts have been made to correlate the base pressure on aerofoil sections at subsonic speeds in terms of the boundary-layer thickness[11], or just the ratio of trailing-edge thickness to chord[3]. It would seem that even in steady flow the base pressure must depend to some extent on both of these factors and the section geometry also. Allowing in addition for the vortex street, however, the problem is complicated still further. It will be shown from the results of the present experiments that the base pressure depends critically on the structure and strength of the vortex street, and that for a given aerofoil section shape and boundary-layer thickness the base pressure can be changed by modification of the base configuration (a rear cavity, a splitter plate, etc.). Thus the prospects of deriving a really satisfactory correlation of base pressures (let alone a reliable analysis) would appear to be remote.

This may not, however, be an acute problem in the context of the design of suitable blunt-trailing-edge aerofoil sections. The existence of the vortex street involves a high drag on account of the momentum loss associated with the concentrations of vorticity. Consequently, for practical purposes the aim is not, primarily, the prediction of the base drag in the presence of the street, but the development of methods of eliminating the periodicity. If this can be done the drag will be reduced and, also, calculation methods based on a steady-flow model would appear to be applicable.

1.3. A major purpose of the series of tests reported in the present paper is to investigate the characteristics of the base flow associated with a blunt-trailing-edge section at subsonic speeds and the part played by the vortex street in the determination of the base pressure. This is assessed by comparison with the results for the steady base flow downstream of a backward-facing step. Observations are also made of the development of the flow pattern associated with the collapse of the vortex system near sonic speed.

A further purpose is to study the modification of the structure of the vortex street, brought about by the attachment of a splitter plate to the base, in the context of its effect on the base pressure, the thickness of the wake and the vortex-shedding frequency. Some interesting relations are shown to exist between these factors. It will be seen that there is a distinction between the results for 'short' splitter plates and those for 'long' splitter plates, and that the effectiveness of a splitter plate in reducing base drag does not necessarily increase with length. In addition to the fairly detailed results for splitter plates two short tests are reported showing the effect of alternative base configurations. A trailing-edge cavity is seen to be beneficial as regards base pressure and this result is interpreted in terms of current knowledge of 'trapped vortices'[15]. On the other hand a rounded trailing edge cannot be relied upon to give a reduction in base drag as compared with a 'square' trailing edge, and in certain conditions is found to be significantly worse.

Aside from the purpose of producing a set of results for comparison with those of the blunt-trailing-edge models, the tests on the rearward-facing step have an important function in their own right. Detailed pressure distributions on the surface downstream of the step are submitted as a basis for the discussion of the reattachment of the separated shear layer. The actual reattachment point (the point at which the surface shear changes sign) is located on the downstream surface in relation to the reattachment pressure rise. Some of these results were referred to in Ref. 10 where it was shown that, in the steady base flow, the pressure rise at reattachment plays an important part in the determination of the base pressure. As an example it was pointed out that the transonic fall in base pressure can be associated with the change from a subsonic- to a supersonic-type reattachment, and that its extent, and the Mach number at which it occurs, can be correlated directly with the development of the reattachment process. The main points of these results are summarised in the present paper.

2. *Experimental Details.*

2.1. *The Tunnel Facility.*

The tests were carried out in the N.P.L. 18 in. × 14 in. High-Speed Wind Tunnel in the induced-flow configuration. The tunnel was fitted with slotted-wall transonic liners[16] of one-eleventh open-area ratio. The solid blockage of the model was about $3\frac{1}{2}\%$; no corrections have been made for boundary interference and the values of free-stream Mach number (M_∞) quoted may therefore be subject to slight inaccuracies. In this respect, however, it should be noted that the comparatively large open-area ratio of the ventilated walls would be likely to minimise the blockage effects on regions of separated flow[17].

With one exception all the tests were made at a constant tunnel stagnation pressure of 31 in. mercury (absolute); the stagnation temperature was close to ambient atmospheric temperature and probably lay in the range 0 to 20°C. The chord Reynolds number was a function of Mach number as is shown in Fig. 1.

2.2. *The Model.*

The initial series of tests was made using the blunt-trailing-edge section shown diagrammatically in Fig. 2. The chord of the model was 6 in., made up of a single-wedge forebody (8·6° total included angle, approximately) 4 in. long, and a 2 in. parallel-sided afterbody. The thickness of the afterbody was 0·6 in., giving a ratio of trailing-edge thickness to chord equal to 10%. The position of pressure tappings on the afterbody and the base is indicated in Fig. 3.

The model was two-dimensional, completely spanning the width (14 in.) of the test section, and was mounted in glass panels fitted in turn-tables for incidence adjustment (Fig. 4).

For subsequent tests the basic model was modified as follows:

(i) A backward-facing step model was formed by the attachment to the lower part of the base of a flat plate 0·3 in. thick and 11·5 in. long also spanning the test section (Fig. 5). The plate was supported on brackets fixed to the side walls of the tunnel, and the incidence of the model could not be varied from zero. The plate was attached in one position relative to the basic model giving a step height of 0·3 in. The junction of the plate and the model was sealed with 'Araldite'. The trailing edge of the plate was chamfered on the lower surface to avoid the introduction of an unacceptable interaction between the flow over the step and that associated with another base.

Pressure tappings were disposed along the centre-line of the surface downstream of the step.

(ii) Wake interference could be introduced by the attachment of splitter plates to the base of the basic model (Fig. 6). The splitter plates, which were cut from 0·040 in. thick spring steel sheet, were provided with tongues for insertion into slots milled in the afterbody on the centre-line of the base. The tongues were 3 in. long in the spanwise direction and were positioned near the tunnel side walls. The centre section of the splitter plates was unsupported, a nominal clearance of 0·010 in. being left between them and the base of the model. Six different lengths of splitter plate were tested: 0·3, 0·6, 0·9, 1·2, 1·8 and 3·0 in., corresponding to $\frac{1}{2}$, 1, $1\frac{1}{2}$, 2, 3 and 5 times the trailing-edge thickness respectively. The longest splitter plate was found to flutter and was supported at its trailing edge by wires attached to the tunnel walls. The shortest splitter plate (0·3 in.) was restrained by two short lengths of 0·060 in. square section cemented to the base near the mid-point of the span but clear of the pressure tappings. These are visible in the flow photograph (Fig. 38). The intermediate-length splitter plates were found to be sufficiently rigid and required no further means of support.

(iii) The effect of trailing-edge geometry was investigated by the attachment of alternative base sections (Fig. 7) to the afterbody of the basic model. The first consisted of a semi-circular cylindrical section of 0·3 in. radius. A single pressure tapping was provided on the centre-line. The second consisted of a fabricated channel section to provide a trailing-edge cavity. The walls forming an extension of the surface of the afterbody were 0·060 in. thick, and no attempt was made to profile either the external surface or the shape of the cavity. The chordwise depth of the cavity was equal to the base height, 0·6 in. Together with the vertical wall of the channel section the overall chord of the model with this base configuration was approximately 6·85 in. Care was taken to prevent leaks into the cavity. A single pressure tapping was again provided on the centre-line of the base.

2.3. *Pressure Measurement.*

At Mach numbers of 0·4 and above the pressures on the surface and the base of the model were measured using a standard 30 in. mercury-manometer bank with the sump maintained at a pressure equal to the tunnel stagnation pressure. At Mach numbers from 0·2 to 0·4 the base pressure was measured relative to the ambient static pressure in the test section by means of a Wallace and Tiernan pressure gauge, model FA145. This instrument could be read to an accuracy of 0·1 in. water.

2.4. *Oil-Flow Patterns.*

An oil-flow technique was used to locate the reattachment point on the downstream surface of the step model. The mixture used consisted of 'Evco 4' (50 gm), titanium oxide (25 gm) and lauric acid (3 gm). 'Evco 4' is a product made by Edgar Vaughan and Co. Ltd., Birmingham.

2.5. *The Stroboscope.*

The formation of the vortex street was observed by means of a stroboscope operated in conjunction with the schlieren optical system. The beam from a continuous light source was interrupted by a rotating slotted disc (*see* photograph, Fig. 8) driven by an electric motor. By control of the motor speed the light beam could be interrupted at a frequency equal to or near the shedding frequency of the vortices. The light passing through the test section of the tunnel was then focused in the usual way[18] on to a ground-glass screen, allowing direct inspection of the flow. A technique was also investigated for photographing the image, using shutter speeds as low as 1/50th sec.

The speed of rotation of the slotted disc was measured using a calibrated E.M.I. flashing-light stroboscope (type 6) illuminating a single white band painted on the disc. The maximum frequency of operation of this instrument was 1 kc/s. By the use of discs with different numbers of slots it was possible to scan shedding frequencies from 1 kc/s to about 17 kc/s. The system was sufficiently developed for it to be a straightforward matter to distinguish between the shedding frequency and the second and higher harmonics in most cases.

When the screen was viewed visually the best results were obtained using a vertical knife-edge cut-off in the schlieren system rather than a graded filter since the maximum sensitivity was required. Some tests were also made using a colour filter. Although this incurred some loss of sensitivity it would appear to be ideal for demonstration purposes.

2.6. *Date of Tests.*

The experiments were carried out between October, 1961 and June, 1962.

3. *Tests on a Blunt-Trailing-Edge Section.*

3.1. *Boundary-Layer Conditions.*

The basic blunt-trailing-edge section (Fig. 2) was tested over a Mach number range of $0 \cdot 2$ to $1 \cdot 12$. At a constant tunnel stagnation pressure of 31 in. mercury the Reynolds number based on the chord increases (Fig. 1) from about $0 \cdot 8 \times 10^6$ at $M_\infty = 0 \cdot 2$ to $2 \cdot 7 \times 10^6$ at $M_\infty = 1 \cdot 12$. No roughness band was used on the model to fix transition but surface oil-flow patterns indicated that at Mach numbers of $0 \cdot 4$ and above the flow in the boundary layers was turbulent at the trailing edge.

Typical boundary-layer velocity profiles derived from pitot traverses are illustrated in Fig. 9 for a Mach number of $0 \cdot 8$, and the variation of boundary-layer thickness with Mach number is shown in Fig. 10. A point 1 in. upstream of the trailing edge was chosen as the measuring station since it will be seen (Fig. 39) that the surface pressure at that point was relatively insensitive to the conditions on the base. Therefore the measured boundary-layer thicknesses are probably representative of most of the conditions under which the subsequent tests on the modified model were carried out.

3.2. *Surface Pressures on the Afterbody.*

The pressure distributions on the surface of the model at zero incidence ahead of the base are illustrated in Fig. 11. At subsonic speeds, up to a Mach number of about $0 \cdot 8$, the pressure falls progressively as the trailing edge is approached, indicating a significant degree of upstream influence from conditions on the base. Over this speed range the pressure coefficient at a given point on the afterbody is seen to be fairly insensitive to variation of Mach number (Fig. 13). At a Mach number of about $0 \cdot 8$ a shock wave develops immediately downstream of the shoulder of the model (i.e. the intersection of the wedge forebody and the parallel afterbody), (Fig. 14b) and, with increase of Mach number from this condition, the shock passes rapidly rearwards giving rise to the small spacial fluctuations of surface pressure on the afterbody seen in Fig. 13. When the shock reaches the trailing edge (Fig. 14c) and supersonic flow is established over the afterbody, the sonic point being located at the shoulder, the upstream influence from the base is largely suppressed. The adjustment in pressure at the trailing edge then takes place through a centred expansion (*see* Figs. 14d and e, e.g.), and what cushioning effect remains is provided by nothing more than the small changes in the displacement thickness of the boundary layer ahead of the base.

The effect of incidence on the pressure distributions on the afterbody is illustrated in Fig. 12.

3.3. *The Base Pressure.*

The spanwise uniformity of the base pressure across the model was found in all cases to be good (Fig. 15) and at supersonic speeds no measurable variation could be detected at distances up to 2·5 in. from the centre of the span. At a Mach number of 0·8 the spanwise variation of base pressure was further investigated by recording the pressures sensed by a pitot probe traversed along the base 0·010 in. from the model. Good correlation was obtained between the probe readings and the base pressures measured at tappings on the model.

At subsonic speeds the sectionwise variation of base pressure, i.e. that in a direction perpendicular to the span, was more pronounced, the peak suction occurring on the centre-line of the base (Fig. 16). With the limited number of pressure tappings provided on the base it was not possible to estimate the mean base pressure reliably and for the purposes of comparison between one test and another, the pressure recorded at hole 6 (Fig. 3) on the centre-line is used. At a small angle of incidence the peak suction on the base occurred at a point towards the upper surface (Fig. 16). As soon as supersonic flow was established over the surface of the afterbody the sectionwise variation of base pressure, at both zero and 2° incidence, disappeared.

In the subsonic range the base flow is dominated by the periodic formation and shedding of eddies into the wake (Fig. 14a). The base-pressure coefficient on the section is low, (indicating a high drag), falling from $-0 \cdot 6$ at low speeds to about $-0 \cdot 7$ at a Mach number of 0·8. This progressive decrease in base pressure is possibly associated with the effect of compressibility on the vortex street, and will be seen (Section 3.9 below) to be reflected in a slow increase in the thickness of the wake. The small rise in base pressure at a Mach number of about 0·85 (Fig. 13) is apparently related to the similar effect which was observed in the surface pressures upstream of the base at a slightly lower Mach number. It can therefore be concluded that the local rise in base pressure is caused by the presence of the shock wave on the surface immediately upstream of the base. [In the present tests this effect is not very significant, but there is evidence from other tests[3, 9, 19] that in cases where the trailing-edge thickness is small quite substantial increases in base pressure can take place under equivalent conditions. If, in the case of sections of small trailing-edge thickness, this effect persists even when measures have been taken to suppress the vortex street, it might possibly be exploited in aerofoil section design. A particularly attractive feature of this effect is that, since it appears to be induced by the development of shock waves, the rise in base pressure tends to some extent to alleviate the drag rise.]

The arrival of the shock wave at the trailing edge of the section and the establishment of supersonic flow over the afterbody is not observed to bring about an immediate suppression of the periodic effects. The present tests indicated that at Mach numbers between 0·9 and 0·975 the shocks trail behind the section at the ends of short well-defined shear layers extending downstream from the separation point on each surface. In this condition there appears to be a complicated interplay between the movements of the shear layers and trailing shocks, and the formation of the vortices (Fig. 17a). Over this short Mach number range the base pressure coefficient is seen to fall rapidly (Fig. 13), reaching a minimum of $-0 \cdot 90$.

This is followed by a significant change in the flow pattern that marks the end of the régime in which the periodic effects and vortex shedding play such a dominant rôle and the beginning of that in which the flow approximates fairly closely to steady conditions. In the present tests this change was, as far as could be judged, discontinuous with a rise in the base pressure coefficient from $-0 \cdot 9$ to $-0 \cdot 825$. In this second régime, which is characteristic of the whole of the supersonic speed range, the shear layers springing from the separation points deflect sharply at the trailing edge to converge to a narrow waist a short distance downstream (Figs. 17b, c). Over a short Mach number range near $1 \cdot 0$ (Fig. 17b), the trailing shocks are bifurcated. A few calculations indicate that at this condition the base pressure is too low for the supersonic flow adjacent to the free shear layers to be deflected back into the stream direction by single oblique shocks. Thus it would seem that in this way the criterion proposed in an early paper by Chapman[20], for estimating the minimum base pressure which can be supported by a two-dimensional base flow, can be evaded. At Mach numbers a little in excess of $1 \cdot 0$ the base pressure (Fig. 13) has risen above the value which can be accommodated by a single oblique shock and the more familiar supersonic base-flow pattern (Figs. 14e, 17c) is established.

With increase of Mach number, from that at which the transition to steady flow takes place, the base-pressure coefficient rises (Fig. 13); and appears to continue rising through the supersonic speed range although the ratio of the base pressure to the free-stream static pressure falls towards zero as the Mach number is increased[3].

The schlieren photograph (Fig. 17b) of the base flow at $M_\infty = 1 \cdot 0$ indicates some persistence of the periodic effects in the wake, although on a small scale compared with the case at Mach numbers below the transition (Fig. 17a, e.g.). There is evidence that concentrations of vorticity can be detected in the wake behind blunt-trailing-edge sections throughout the supersonic range[3, 21]. However, their effect is apparently small, and it will be shown (Section 4.2 below) that the influence of the unsteadiness on base pressure decays rapidly as soon as sonic velocity is reached in the free stream. The discrepancy which was pointed out in Ref. 3 between the measured base-pressure values at low supersonic speeds and the values predicted by the theory of Korst[22] and others has now been explained[10] not in terms of the persistence of periodic effects in the wake but in the failure of the steady-flow theories. A further indication that in the low supersonic range the flow approximates to the steady base flow assumed in the theory is given by the collapse of the base-pressure readings recorded at different points on the base to a single curve (Fig. 13). In contrast to the case at subsonic speeds the pressure is constant over the base indicative of a region of sensibly dead air in the initial part of the wake.

3.4. *Effect of Reynolds Number.*

At a Mach number of $0 \cdot 8$ the tunnel stagnation pressure was raised to increase the test Reynolds number. It is seen from Fig. 18 that the effect of doubling the chord Reynolds number was to increase the base-pressure coefficient by less than 1%.

3.5. *Effect of Incidence.*

The pressure distributions on the afterbody of the model at 2° incidence are illustrated in Fig. 12.

The schlieren photographs (Figs. 19a to e) of the flow over the model at 2° incidence exhibit no major difference in the structure of the wake and the vortex street is still strong at subsonic speeds. The slight asymmetry was seen (Section 3.3 above) to be reflected in the sectionwise pressure distribution across the base, the peak suction occurring not on the centre-line but displaced towards the upper surface. At subsonic speeds the base pressure is found to be slightly higher on the model at 2° incidence than at zero incidence (Fig. 20a), but the small increase in base pressure at high subsonic speeds is noticeably less pronounced. In the steady-flow régime at sonic and supersonic speeds, no variation of base pressure could be detected for small changes of incidence.

A rise in base pressure with increasing incidence (Fig. 20b) is typical of two-dimensional sections at subsonic speeds[7, 9, 23], and is possibly associated with the increase in the thickness of the boundary layer on the upper surface (*see* Fig. 19).*

3.6. *Comparison with Results of Other Tests.*

A comparison was made in Ref. 3 between the base pressure measured on the present basic model and the results of other wind-tunnel and free-flight tests.

Wake Exploration.

3.7. *Static Pressure.*

The variation of static pressure along the centre-line of the wake behind the basic model was investigated using a standard static probe aligned in the stream direction. No attempt was made to minimise the effect of instantaneous probe yaw induced by the cross flows in the wake at subsonic speeds, either by the appropriate orientation of a probe with a single static hole[24], or by the use of a spade-shaped static probe[25]. For this reason, and since the interpretation of the readings of a probe set in an unsteady flow is in any case difficult, the results (Fig. 21) should be regarded as qualitative rather than quantitative.

At subsonic speeds it is seen that the static pressure falls rapidly away from the base reaching a minimum at a distance downstream equal to about half the trailing-edge thickness (Fig. 21). The existence of this low pressure 'trough' has been observed in a number of tests on the flow past bluff bodies[24, 25, 26] and is believed to coincide with the point at which the vortices form. The value of the pressure coefficient in the trough appears to decrease with an increasing degree of bluffness of the section, and hence, presumably with increasing strength of the vortex street. For example, in the present test, the minimum value of C_p is about $-1 \cdot 0$, compared with $-1 \cdot 4$ for a circular cylinder[27] and $-2 \cdot 3$ for a flat plate normal to the stream[25].

Downstream of the trough the static pressure rises again and levels out at some value below ambient static pressure. The presence of such a pressure 'plateau' along the centre-line of the wake, as distinct from a progressive increase of the static pressure with distance downstream of the section, is indicative of the existence of a vortex street. [It can be shown theoretically that the static pressure along the centre-line of a vortex street is lower than free-stream static pressure by an amount depending on the strength of the street.] Moreover the eventual decay of a vortex street is marked by the end of the plateau and the return of the static pressure to the free-stream value. The present static-pressure exploration was not continued sufficiently far downstream to show this effect, but it is evident from the results of Ref. 27.

With increase of Mach number into the régime in which trailing shocks begin to develop (*see* Section 3.3 above) the point at which the vortices form is pushed downstream (Fig. 17a) and the

---

* In contrast to this, however, the base pressure on a slender delta wing model[6] was observed to fall with increasing incidence, although this effect may have been caused by the development of the leading-edge vortex.

position of the low pressure 'trough' is similarly displaced. At a Mach number of 0·95, for example, the minimum static pressure is reached at a distance from the base equal to nearly one base-height (Fig. 21).

At Mach numbers above the transition to the 'steady' base flow (0·975 on the present model), the presence of a low pressure trough in the wake is not easy to discern (Fig. 21), and the constant-pressure region extending downstream from the base, indicating a region of semi-dead air, is quickly established. Moreover, the static pressure in the wake subsequently approaches the free-stream value without any intermediate plateau. Thus it would seem that, while there is evidence of the persistence of discrete eddies in the wake at supersonic speeds, their strength must be reduced to such an extent that the wake displays few of the characteristics of a fully-developed vortex street.

3.8. *Pitot Pressure.*

An extensive survey of the wake behind the basic model was made using a pitot probe aligned in the stream direction, and the results are presented in Figs. 22a to e in terms of a parameter

$$\frac{H_0 - H}{H_0 - p_\infty},$$

where H is the pitot pressure, H_0 the stagnation pressure and p_∞ the ambient static pressure. Using these curves it is instructive to plot contours of constant pitot pressure and reconstruct the flow field. This has been done in Figs. 23 and 24 for Mach numbers 0·8 and 1·0 respectively.

At subsonic speeds it was considered useful to derive some measure of the variation of wake thickness with distance downstream of the base. For this purpose the wake thickness at a given station was defined as the distance between points on opposite sides of the centre-line at which the value of the parameter

$$\frac{H_0 - H}{H_0 - p_\infty}$$

was equal to half the value on the centre-line at that station. For a Mach number of 0·8 the locus of points satisfying this condition is traced in Fig. 23. It is seen that for a short distance from the base the wake converges and reaches a minimum thickness at a point a little further downstream than the position of the low-pressure 'trough' (*see* Section 3.7 above). From this station onwards the wake spreads slightly and then continues for a considerable distance with an almost constant thickness. This region probably corresponds to the fully developed vortex street and the pressure 'plateau' referred to above.

It was thought that the wake thickness in this region could be considered as a convenient measure of the equivalent 'width' of the vortex street, i.e. the distance between the rows of vortices. Accordingly, a thickness h' (Fig. 25) was defined, being the thickness of the wake at a station 2 in. (3·33 h) downstream of the base. (*See also* Fig. 23.)

At a Mach number of 1·0, Fig. 24 illustrates the contours of constant pitot pressure in the wake and the surrounding flow field, in the 'steady flow' régime. This diagram should be compared with the schlieren photograph (Fig. 17b) taken under the same conditions. The positions of the trailing-edge expansion, the boundary of the wake, and the trailing shock system are clearly indicated. Also it is interesting to note the persistence of the shear layer extending downstream from the junction of the two branches of the trailing shock. Part of this discontinuity can be discerned in the schlieren photographs (Figs. 14d, 17b).

3.9. *Wake Thickness.*

The wake thickness ratio h'/h, defined above (*see* also Fig. 25), was measured at several conditions and its variation with Mach number is shown in Fig. 26. Through the régime in which periodic effects are predominant (i.e. for Mach numbers up to $0 \cdot 975$), the wake thickness exhibits largely the same behaviour as the base-pressure coefficient. At the lower subsonic speeds the slow rise in h'/h reflects the similar increase in the base drag. The local decrease in base drag at $M_\infty = 0 \cdot 9$ is reflected in a small decrease in h'/h, but the latter extends from a slightly lower Mach number. However, this could possibly be explained insofar as the wake experiences changes of conditions not only on the base but also on the surface of the body ahead of the base. It will be recalled (*see* Section 3.2 above) that the small rise in base pressure was anticipated, in terms of increasing Mach number, by similar fluctuations of the surface pressure on the afterbody. Thus the response of the wake to the integrated effect of these changes in pressure could well correspond to the observed behaviour.

Following the decrease in base drag $(-C_{pb})$ and the wake thickness, associated with the rearward movement of the shock over the afterbody, the Mach number range in which the shocks trail behind the section in an unsteady condition was seen to be marked by an abrupt decrease in base pressure (Section 3.3 above). While the free shear layers do, to a small extent, converge after the separation points (Fig. 17a), the wake spreads out downstream of the trailing shocks, and the thickness of the wake at the reference station, 2 in. from the base, increases quite sharply (Fig. 26).

The transition from the predominantly unsteady-flow régime to that of the steady base flow, at a Mach number of $0 \cdot 975$ on the present model, is accompanied by a dramatic decrease in the thickness of the wake. While the rise in the base-pressure coefficient at the discontinuity amounted to no more than 10%, the wake thickness falls from $1 \cdot 25$ times the base height to about half this value. The interpretation of this change is quite clear from the schlieren photographs (Figs. 17b, c), where it is seen that the reduction in wake thickness is made possible by the larger angle of deflection of the shear layers at the trailing edge and, more important, by their increased length which brings them to a narrow region of confluence. The break in the close relationship between base pressure and wake thickness that has held up to this point is a further reflection of the change from subsonic to supersonic conditions in the region of confluence.

With increase of Mach number, from that at which the transition to steady flow takes place, the wake thickness is observed to decrease still further (Fig. 26).

3.10. *Vortex Shedding Characteristics.*

It has in the past been asserted by certain authorities that the existence of turbulent motion in the boundary layer at the separation points on a body is incompatible with the development of a regular vortex street[11], (*see* Section 1.2 above). It will thereby be necessary to state what is meant by a vortex street under these conditions. Over time intervals of the same order, or less than the periodic time of the street, a given section of the wake may not always display regular eddies. Thus flow photographs taken using a spark light source (such as those included in the present paper) may depict the flow in the wake as being largely random in character as distinct from periodic. For this reason single flow photographs cannot be submitted as reliable evidence of the *absence* of a vortex street (although of course many of the photographs offer positive evidence of the presence of vortex streets).

Over a time interval large compared with the periodic time of the motion, the flow in the wake will be observed to be strongly and regularly periodic. These considerations led to the choice of a stroboscopic device for surveying the wake. The arrangement (*see* Section 2.5 above) consisted of a conventional schlieren optical system[18] illuminating a ground-glass screen, in which the light beam was interrupted at a frequency which could be adjusted to equal the frequency at which pairs of vortices were shed into the wake. In this way the process of the formation and development of the vortex street could be inspected visually. It was felt that even from the point of view of frequency measurement this method compared well with systems involving electrical recording and frequency spectrum analysis. Moreover, as regards interpretation of the data and gaining some insight into the mechanism of vortex formation, the present system had clear advantages. The only important disadvantage which was apparent was the lack of any means of measuring the amplitude of the fluctuations of the flow parameters in the wake.

The vortex shedding frequency measurements are presented in the form of a Strouhal number S, where

$$S = \frac{nh}{u_\infty}, \tag{1}$$

n is the shedding frequency, h the base height, and u_∞ the free-stream velocity. The variation of the Strouhal number with Mach number for the basic blunt-trailing-edge model is shown in Fig. 26. At Mach numbers up to $0 \cdot 9$ the Strouhal number remained constant, to within the limits of the accuracy of measurement, at a value of $0 \cdot 25$. The development of trailing shocks behind the section, which was seen to be associated with a fall in the base pressure and an increase in the wake thickness (Sections 3.3, 3.9 above), is marked by a progressive increase in the Strouhal number to about $0 \cdot 31$.

The transition from the unsteady-flow régime to that in which the base flow is predominantly steady, which was seen to be accompanied by a discontinuity in the base pressure and the wake thickness, gives rise also to a discontinuous increase in the shedding frequency. At Mach numbers above the transition ($0 \cdot 975$ on the present model) the vortex street was observed to be less strong, but the Strouhal number is then in the region of $0 \cdot 4$ (Fig. 26), and falls only slowly with increase of Mach number.

From their extensive data on the vortex-shedding characteristics of bluff sections, Fage and Johansen observed that the Strouhal frequency appeared to increase inversely as the thickness of the wake[28], and that a more fundamental Strouhal number could be formed using the wake thickness as the reference dimension. Using the measured values of h'/h, a Strouhal number S' is considered where

$$S' = \frac{nh'}{u_\infty} = \frac{h'}{h} S. \tag{2}$$

The variation of this wake Strouhal number with Mach number is illustrated in Fig. 26. It is seen that the behaviour of this quantity follows, even more closely than the wake thickness alone, the variations of the base drag $(-C_{pb})$.

4. *The Flow Past a Step.*

A diagram of the backward-facing step model is shown in Fig. 5. The height of the step was equal to half the trailing-edge thickness of the basic model, and will be denoted by $\frac{1}{2}h$ for consistency with the previous results.

4.1. A careful survey of the flow downstream of the step using the stroboscope unit (*see* Sections 2.5 and 3.10 above) failed to reveal any evidence of periodicity. This is not to say that the flow is entirely steady in character and flow visualisation techniques have indicated the existence of eddies moving downstream in the viscous layer[29]. However, it would seem that such disturbances are random in character and for the purposes of our present discussion can be grouped with normal turbulence effects. Thus it will be convenient to refer to the base flow behind a step as 'steady' although the term should be interpreted carefully.

4.2. *The Base Pressure.*

The variation of the base pressure on the face of the step with Mach number is shown in Fig. 27. Through the subsonic range the base-pressure coefficient remains roughly constant at a value near $-0 \cdot 2$. At high subsonic speeds as soon as sonic velocity is reached at the separation point, and simultaneously at the reattachment point, the base pressure falls abruptly approaching the values measured on the basic blunt-trailing-edge model. This effect is similar to the sharp decrease in base pressure which is observed at transonic speeds on aerofoil sections for which the ratio of trailing-edge thickness to chord is small (*see* Ref. 3). Indeed the fact that this decrease in base pressure can be reproduced in a test where the periodic phenomena are inhibited is ample evidence of its being a steady-flow effect.

Comparing the results for the step and for the basic model (Fig. 27) it is noted that throughout the subsonic speed range there is a large discrepancy between the base pressures in the two cases. At a Mach number of $0 \cdot 8$, for example, the base-pressure coefficient on the step is $-0 \cdot 23$ as against $-0 \cdot 75$ on the isolated section. These figures give some impression of the proportion of the drag of an isolated section which can be attributed to the existence of the vortex street. It will be recalled that Hoerner[30] analysed data on the base drag of blunt-trailing-edge aerofoils at low speed and demonstrated that the values were in every case higher, under equivalent conditions, than the measurements of the drag of sheet metal joints (small rearward-facing steps) by Wieghardt[31]. In Wieghardt's tests the ratio of boundary-layer thickness to step height was much larger than in the present work. Nor is it possible to compare the base pressure measured on the present model with the results of Tani *et al*[29], since in the latter tests the true ambient static pressure was not recorded. The data were presented in the form of pressure coefficients relative to the static pressure measured at a point on the model within the pressure field of the step, and using the value of the 'free-stream' velocity also computed from this pressure reading. For this reason some of the conclusions drawn from the investigation, for instance, that the base pressure was relatively insensitive to the thickness of the approaching boundary layer, were based on a misinterpretation of the results and are not valid.

4.3. *Surface Pressures on the Upstream Surface.*

The pressure distributions on the surface of the model upstream of the step are shown in Fig. 28, and may be compared with the results for the basic model (Fig. 11). It will be noted that, at the higher Mach numbers, when the flow over the afterbody is locally supersonic the pressures over the afterbody are much the same in Figs. 11 and 28, except in the immediate vicinity of the separation point. At lower speeds when the flow is locally subsonic the effect of changes of pressure on the base is felt at considerably larger distances upstream of separation. This point will be touched on again in Section 5.2 below. It is also interesting to note that at a Mach number of $0 \cdot 8$

the surface pressure appears to fall to a slightly lower value immediately upstream of the step than on the base itself. This effect was also observed at $M_\infty = 0 \cdot 6$ and is suggested by the form of the distribution at $0 \cdot 4$. It could be argued that the small rise in pressure at the corner is associated with the separation of the boundary layer. If this is so the fact that it was not noticed in the case of the basic section (Fig. 11) might be explained either by its being obscured by the rather more abrupt expansion, or even possibly, insofar as the separation is modified to some extent by the unsteady effects.

Over a certain range of Mach number, near $0 \cdot 9$, the pressure on the upstream surface is lower than the base pressure and the adjustment at the corner is represented by a compression instead of the more familiar expansion (Fig. 28). A weak shock can in fact be detected in the neighbourhood of the separation point in the corresponding schlieren photograph (Fig. 29c). At a Mach number of unity the pressure distribution ahead of the step (Fig. 28) follows the typical pattern for supersonic base flow.

4.4. *Surface Pressures on the Downstream Surface.*

The pressure distributions on the surface of the model downstream of the step are shown in Fig. 30. In contrast to the low pressure 'trough' observed in the wake behind the basic model at subsonic speeds, the surface pressure remains almost constant for a short distance downstream of the step (Fig. 31), indicating the presence of a region of semi-dead air. Thus not only does the existence of a vortex street, in the case of the basic blunt-trailing-edge section, lead to a decrease in the base pressure but it involves in addition a substantial modification of the pressure field in the wake. The stability of the base flow behind an isolated section at supersonic speeds brings about a greater degree of equivalence and the pressure distributions in the two cases are then essentially similar.

The low pressure in the dead-air region is followed, with increasing distance from the step, by a sharp pressure rise which is associated with the reattachment of the separated free shear layer to the downstream surface (Fig. 30). It would appear that an adequate model of the subsonic base flow behind a step can be constructed considering the separation of the boundary layer at the corner, the development of the free shear layer along the edge of the dead-air region and the subsequent reattachment process. This flow model was discussed in Ref. 4 as a basis for the analysis of steady subsonic base flow. A theoretical investigation of the growth of the free shear layer from a turbulent boundary layer at separation was presented in Ref. 32. In the case of the flow past a step the steady-flow model appears to be valid throughout the Mach number range and such effects as occur at transonic speeds, although very significant in terms of base pressure for example, will be seen to be the result of changes of detail rather than an essential modification of the flow pattern.

Fig. 30a shows that at subsonic speeds the pressure does not rise monotonically from the value in the dead-air region with distance from the step but exhibits the characteristic 'overshoot'. This effect is typical of the subsonic reattachment[29, 48] and can be related to the concave curvature of the streamlines in the external flow and an associated local increase in the stream-tube area (Fig. 32a). [The pressure distributions downstream of the spoiler in Ref. 49 were probably terminated too soon to show the overshoot.] With the establishment of a supersonic reattachment the concavity of the streamlines is no longer associated with a locally high pressure (Fig. 32b), and at the highest Mach number reached in the tests, $1 \cdot 10$, the overshoot had almost disappeared (Fig. 30b).

4.5. *The Reattachment Process.*

The actual reattachment point which is a point of zero surface shear stress was located on the downstream surface by an oil-flow technique (*see* Section 2.4 above). The length of the separation bubble, i.e. the distance of the reattachment point downstream of the step, is found to vary with Mach number according to Fig. 33. Through the subsonic range the length of the bubble, and hence also of the free shear layer adjacent to it, increases with Mach number up to a value equal to about eleven times the height of the step at $M_\infty = 0 \cdot 975$. At higher Mach numbers the free shear layer is observed to deflect sharply at the corner (Figs. 29e, f) and the length of the bubble decreases accordingly (Fig. 32). At supersonic speeds theoretical models of base flow usually relate the geometry of the dead-air region to the height of the step and the Prandtl-Meyer angles corresponding to the local Mach number of the flow adjacent to the free shear layer and the free-stream Mach number. In these terms the distance of the reattachment point downstream of the step should be given by

$$\frac{l}{\frac{1}{2}h} = \cot\,(\nu_s - \nu_\infty)\,,$$

where M_s is the Mach number reached by allowing the fluid in the free stream to expand isentropically from pressure p_∞ to pressure p_b. It is seen from Fig. 33 that the values of h derived from this expression are a good approximation to the measured length of the region of separation.

With the reattachment point located on the downstream surface, its position with respect to the pressure rise through the reattachment region can be determined. The positions of the reattachment point are indicated on the surface pressure distributions in Fig. 30.

An essential feature of the reattachment process lies in the way in which the pressure recovery, from the base pressure to free-stream static pressure, is disposed upstream and downstream of the reattachment point. Fig. 34 shows that the upstream pressure recovery $(C_{pr} - C_{pb})$ is relatively constant, lying between $0 \cdot 2$ and $0 \cdot 4$ over the whole Mach number range. In contrast to this the downstream pressure recovery $(-C_{pr})$ exhibits much larger excursions particularly at transonic speeds.

The former effect is to be expected on the basis of the flow model discussed in Ref. 4. According to this model the pressure rise up to the reattachment point is associated with the retardation to rest of the fluid on the mean dividing streamline. This, in turn, depends chiefly on the length of the separated shear layer—except if this length is large compared with the boundary-layer thickness at separation[32] when the velocity on the dividing streamline is substantially constant. In the present case this condition is in fact satisfied. Thus, neglecting the variations of the velocity on the dividing streamline due to variations in the length of the separated region, and also the less important variations due to changes in Mach number, it can be appreciated that the upstream pressure recovery will not vary greatly over the range of conditions of the experiment. The variations in the downstream pressure recovery account directly for those of the base-pressure coefficient, particularly at Mach numbers near unity.

At subsonic speeds the pressure initially rises downstream of the reattachment point, reaches a maximum and subsequently falls again towards free-stream ambient pressure far downstream (Fig. 30a). But the value of C_{pr} is positive, indicating that the net pressure recovery downstream of reattachment is negative (Fig. 34). As supersonic flow is established, however, the overshoot in the pressure distribution gives way to a monotonically rising pressure (Fig. 30b) and a substantial degree of pressure recovery takes place between the reattachment point and a point far downstream

(Fig. 34). At infinity downstream the pressure must necessarily return to ambient static pressure and therefore the base pressure is forced to decrease considerably in order that this extra pressure recovery can be accommodated. The onset of this effect is of course nothing else than the transonic fall in base pressure. It is something of a paradox that, while most attempts (previous to Ref. 10) to predict base pressures theoretically have been based on the prediction of the pressure rise upstream of reattachment, in this case the whole nature of the variation of base pressure with Mach number depends on the downstream pressure recovery.

It was demonstrated in Ref. 10 on the basis of the present results that once the correct reattachment conditions are taken into account the variation of base pressure with Mach number through the transonic range can be predicted successfully. For this purpose it was found convenient to define a recompression parameter N, where

$$N = \frac{C_{pr} - C_{pb}}{(-C_{pb})},$$

which expresses the position of the reattachment point with respect to the overall pressure rise downstream of the trailing edge. The variation of N with Mach number determined from the present experiments is shown in Fig. 35 together with the variation of base-pressure coefficient indicated by the theory for the empirical values of N.* The agreement between the measured and the computed values of C_{pb} is seen to be very satisfactory.

The pressure recovery which takes place downstream of reattachment in the supersonic base flow is indicative of the continued deflection of the streamlines outboard of the sonic boundary (Fig. 32b). This streamline curvature is apparently made possible by a progressive decrease in the boundary-layer displacement thickness, with distance downstream, from its relatively large value at the reattachment point to a lower value appropriate to the boundary layer at a point of zero pressure gradient. It seems clear, therefore, that the form of the pressure distribution along the surface downstream of the reattachment point is governed by the interaction between the boundary layer and the external stream. In a recent paper McDonald[33] has proposed a simplified analysis of the reattaching boundary layer and, on this basis, has been able to show that base pressures may be predicted at supersonic speeds without appeal to an empirical recompression parameter.

It was pointed out in Ref. 10 that there are grounds for suspecting that the reattachment of a separated shear layer to a solid surface might not be directly equivalent to the confluence of two shear layers as occurs in the wake of a blunt-trailing-edge aerofoil section at supersonic speeds. This becomes important in view of the dependence of the base pressure on the pressure recovery downstream of the reattachment point (or point of confluence). Thus it is necessary to establish whether the values of N derived from measurements on a rearward-facing step model are applicable to a wake flow at supersonic speeds under nominally equivalent conditions. If there is a difference between the two cases it could be expected to be manifest by a difference in the base pressure. Fig. 35 shows that at Mach numbers of 1·05 and 1·10 there is approximately the same difference, 0·06, between the base-pressure coefficients measured on the basic isolated section and the step. At lower Mach numbers, however, down to 0·975, there is a large discrepancy between the base pressures recorded on the two models. While over the Mach number range 0·975 to 1·05 the base

* At Mach numbers up to unity it was also necessary to make use of the measured values of the length of the separated region (Fig. 33).

pressure on the step is falling under the influence of the changing reattachment conditions, the base pressure on the basic model is already at a low value, and rising steadily, as though the value of N had reached its final low level. The implications of this observation need to be investigated, but it would seem that the transition to the 'steady' base flow, in the case of the isolated section, is not immediately accompanied by an adjustment of the base pressure to values equal to those on the step.

5. *The Effect of a Splitter Plate on the Flow Past an Isolated Section.*

5.1. The use of a splitter plate, i.e. a thin two-dimensional flat plate placed in the plane of symmetry of the wake, to modify the process of vortex formation behind bluff sections, has been demonstrated a number of times[13, 14, 27, 34, 35, 36] in tests at low speeds. In cases where the length of the splitter plate has been relatively short compared with the size of the body the formation of the vortex street has not been completely inhibited but substantial reductions in drag have still been achieved[27]. It appears, moreover, that a splitter plate positioned a short distance downstream of the section, i.e. with a small gap between it and the base, can be as effective as one attached to the body[27]. If the length of the splitter plate is sufficient, the stream from each separation point should reattach to it without interference from the other, suppressing the periodicity and transforming the base flow into a type similar to that downstream of a step. However, if the measured lengths of the separation bubble behind the step (Fig. 32), and the linear scale of the pressure distributions (Fig. 30) are taken as a guide it would seem that a completely steady reattachment would require a splitter plate of a considerable length. In fact, in their tests on a flat plate normal to the stream, Arie and Rouse[35] report that a splitter plate ten times the height of the section was necessary before the base pressure was insensitive to further increase of length.

An interesting variation of the splitter plate concept is the use of a jet of air issuing from a narrow slot on the centre-line of the base of a blunt-trailing-edge section. Poisson-Quinton and Jousserandot[38] were able to achieve substantial reductions of the total drag of a truncated aerofoil section at subsonic speeds using this method.

5.2. *The Effect on Base Pressure.*

In the present series of tests the length of the splitter plate was varied from a half, to five times, the trailing-edge thickness (Fig. 6). The variation with Mach number of the base pressure on the model fitted with a splitter plate is illustrated in Fig. 36. It is seen that at subsonic speeds the effect of a splitter plate is to reduce that part of the base drag which can be attributed to the existence of the vortex street, and the curves lie between those for the basic section and the backward-facing step. In the steady base flow the presence of a splitter plate should have no effect, and at supersonic speeds this is seen to be approximately correct for the longer splitter plates. However, the two shortest splitter plates apparently produce a significant decrease in base pressure. This is believed to be due to the excitation of an instability in the separated region, and Fig. 38 shows a direct shadow photograph of a particularly severe case. It is possible that the instability is provoked by the impingement of the reversed flow on the end of the splitter plate.

The effect of variation of base pressure, at a given Mach number, on the surface pressures upstream of the base is illustrated in Fig. 39. The data relate to the basic section with and without a short splitter plate, and the step model.

It will be noted from Fig. 36 that while the effect of a splitter plate at subsonic speeds is to increase the base pressure above the values recorded for the basic blunt-trailing-edge model, the effect does not increase monotonically with the length of the splitter plate. In fact raising the length of the plate from one to two times the base height is seen to result in a marginal decrease in base pressure. The variation of base pressure with splitter-plate length is illustrated in Fig. 40. It is seen that after the initial, fairly rapid, increase of base pressure effected by the shorter splitter plates, there is a significant fall in the base pressure followed by a second rise. For a splitter plate of length about equal to the trailing-edge thickness, the base pressure appears to reach a local maximum, which at low speeds, represents a reduction in base drag ($-C_{pb}$), of more than 50%. This result would suggest that a short splitter plate can offer a simple and convenient method of reducing base drag, and one which would appear to incur few penalties. Similar large decreases in the total drag of a blunt-trailing-edge aerofoil section, fitted with a splitter plate of equivalent length, have been reported by Moulden *et al*[9], and Poisson-Quinton and Jousserandot[38].

When the length of the splitter plate is greater than twice the trailing-edge thickness, the base pressure appears to rise monotonically with increasing length (Fig. 40), although the intervals in length used were not sufficiently small to make this certain. With a splitter plate five base-heights long, the base pressure is seen to be approaching the measured values for the rearward-facing step.

5.3. *'Short', and 'Long' Splitter Plates.*

The form of the curves in Fig. 40 suggests the existence of two flow régimes, one appropriate to 'short', and a second to 'long', splitter plates. Similar effects have been observed by Thomann[14], and by Roshko[24, 27]. In the latter tests a short splitter plate was placed at varying distances behind a section. Roshko reported that there appeared to be a discrepancy between the results obtained with the splitter plate close to the section, and those where it was placed further downstream when it would, in effect, be equivalent to a longer one.

Some indication as to the reasons for the existence of two régimes is given by the schlieren photographs (Figs. 37a to e), taken at a Mach number of 0·4. In the case of the 'short' splitter plates (Figs. 37a, b), the point at which the wake breaks up into discrete vortices is downstream of the end of the splitter plate, and the plate itself appears to lie in a region of relatively dead air. In fact there is some evidence that the point at which the vortices form is displaced downstream by a distance roughly equal to the length of the splitter plate. With the shortest splitter plate ($\frac{1}{2}h$) in position the low pressure 'trough' in the wake was located at a distance h downstream of the base compared with $\frac{1}{2}h$ downstream in the case of the basic section. Thus it would seem that the main effect of the 'short' splitter plates is to displace the point of vortex formation further downstream from the base. A survey of the wake using the stroboscope showed no significant degree of periodicity in the free shear layers passing over the splitter plate.

These effects appear to continue until the length of the splitter plate exceeds the trailing-edge thickness. Between this condition and that at which the length of the splitter plate is twice the base height, a change in the base-flow characteristics takes place. It may be significant to note that half a wavelength of the vortex street is equal to about 1·8 times the trailing-edge thickness.

In the case of the 'long' splitter plates (i.e., $2h$ and longer), the 'dead-air' region does not extend so far from the base (Figs. 37d, c) and the shear layers appear to impinge on, if not to reattach to, the splitter plate. Also it was observed, using the stroboscope, that periodic disturbances were present in the free shear layers from the separation points onwards. Concentrations of vorticity were seen to develop and grow in intensity as they passed alternately along each shear layer over the length of the splitter plate. The fact that the rolling-up of the shear layers into discrete eddies had commenced before any direct interaction could take place between the fluid particles involved and those in the other shear layer, would appear to lend considerable support to the concept of a periodic circulation round the section. The instantaneous shear layer asymmetry associated with the circulation could be regarded as the result of an interaction further downstream.

5.4. *The Effect on Vortex-Shedding Frequency.*

The vortex-shedding frequencies measured on the model fitted with 'short' splitter plates are presented in Fig. 42a. With the splitter plate of length h, at Mach numbers between $0 \cdot 4$ and $0 \cdot 6$, there was evidence of wake periodicity, but it was found difficult to determine the predominant frequency. Outside this range the vortex shedding appeared to be strong and regular and the measurement of the Strouhal frequency was straightforward. In the subsonic speed range the main effect of the splitter plates is seen to be an increase in the shedding frequency above that measured on the basic section. Also it is noted that the Strouhal number is no longer constant with respect to Mach number. At supersonic speeds the test data are submitted but it should be pointed out that the frequencies may well have been influenced by the oscillation of the base flow referred to above (Section 5.2 and Fig. 38). Thus these measurements should be treated with reservation in any discussion of the characteristics of the vortex street.

In the case of the model fitted with a splitter plate of length $3h$ (Fig. 42b), the vortex street was relatively weak but well defined, and the Strouhal number was found to vary smoothly with Mach number. For the splitter plate of length $2h$, however, at Mach numbers below $0 \cdot 7$, the shedding frequency was well defined but did not appear to increase uniformly with Mach number. The scatter of the data points in Fig. 42b should not imply an inaccuracy of measurement but a loss of regularity of the vortex formation process itself. It is noted that this length of splitter plate represents the establishment of the 'long' splitter-plate régime, and the flow could conceivably be in a state of unstable equilibrium.

It would at present be premature to attach too much significance to this apparent instability, and indeed the possibility that the effect represents an irregularity in the measuring equipment cannot be ruled out. Nevertheless it may be instructive to examine the data more closely. In a few cases it is observed that two shedding frequencies are indicated at the same Mach number. Using the stroboscope, the two modes appeared to be excited concurrently and it was possible to tune the device to either frequency at will. It is conceivable that the vortex shedding could have been fluctuating between the two modes with a time scale long compared with the average periodic time of the vortices. The concept that under certain conditions the vortex formation might advance from one discrete mode to another is interesting, and is to some extent in accordance with the suggestions of Shaw[41]. In the context of a section of the type under consideration it would seem that one 'centre of disturbance', to use Shaw's terminology, must be located at the leading edge, and the other two, making up a three-point system, positioned either at the two rear separation points or at symmetrically disposed points in the free shear layers. In either case the mode of acoustic vibration would appear to be restricted to odd harmonics of the fundamental. If the rear centres of disturbance are assumed to lie at the separation points the mode should be equivalent to the 21st harmonic (equal to the ratio of the total perimeter to the base height). If the system should now advance to the next possible mode, this should be the 23rd harmonic and the Strouhal frequency would increase, according to the arguments of Shaw, by 9·5%. In the three cases where dual shedding frequencies were observed the Strouhal numbers were as follows:

M_∞	S_1	S_2	Difference, %
0·25	0·273	0·303	11
0·55	0·245	0·270	10
0·65	0·230	0·250	9

Allowing for the experimental error, especially at the lowest Mach number where the contrast obtained in the schlieren system is poor, the correlation is remarkable.

The variation of the Strouhal number with the length of the splitter plate is illustrated in Fig. 41 for a Mach number of 0·4, in comparison with the results of Thomann[14]. In these latter experiments a single-wedge basic section, of thickness-chord ratio 1/6, was used. It is seen that the lack of continuity between the results for 'short' and 'long' splitter plates is as much a feature of the shedding frequencies as it was of the base pressures. Moreover, the point, in terms of increasing splitter-plate length, at which the change takes place is approximately the same as that determined by Thomann. It is strange at first sight to note that the variations in frequency observed in the present tests appear to be of opposite sign to those submitted in Ref. 14. However, this difficulty can be resolved quite readily.

According to free-streamline theories[42, 43] of the so-called 'parallel-streamline' type, it is a property of sections on which the separation points lie at positions where the surface slope is positive (i.e. where the thickness is increasing downstream), that an increase in base pressure is accompanied by an increase in the wake thickness; the wake thickness, d, in this case being defined as the distance between the free streamlines at infinity downstream. Now it has been shown experimentally[28] that an increase in wake thickness is frequently associated with a decrease in the vortex shedding frequency. Thus for a single-wedge section it would be expected that the effect of a splitter plate, which increases the base pressure, would be to decrease the Strouhal number; just this result was observed in Ref. 14. On the other hand, if separation occurs at a point of negative surface slope (boat-tailed afterbody), the increase in base pressure is accompanied by a decrease in wake thickness, and a corresponding increase in vortex-shedding frequency. Although the present section has a parallel afterbody, the tests indicated that the effect of the attachment of a splitter plate is to decrease the wake thickness (Fig. 43). Thus it would seem that the section exhibits the behaviour of one with separation at points of negative surface slope, and the observed variation of Strouhal number with splitter-plate length is consistent with this suggestion.

5.5. *Further Thoughts on 'Short' and 'Long' Splitter Plates.*

The variations with splitter-plate length of the base-pressure coefficient, the wake thickness ratio, h'/h, and the vortex-shedding frequency are compared in Figs. 43a, b for Mach numbers of 0·4 and 0·8. The shedding frequencies are reduced to the normal Strouhal number, S, and also the Strouhal number, S', based on the wake thickness h'.

The distinction between the 'short' and 'long' splitter-plate régimes is further emphasised by a plot of the base-pressure coefficient against the wake Strouhal number (Fig. 44). In the 'short' splitter-plate régime (assumed to include the basic section), the derivative $\partial C_{pb}/\partial S'$ is positive, indicating that the wake Strouhal number increases with increasing base pressure. However, the increase of the length of the splitter plate from h to $2h$ results in a shift to a second curve of negative slope. It would appear, moreover, that the second curve could be extrapolated back to pass through the data point representing the basic section (denoted by a filled symbol in Fig. 44). Thus the data relating to 'short' and to 'long' splitter plates appear to lie on two curves which intersect at the condition relating to zero splitter-plate length. This effect is observed for each of the Mach numbers $0 \cdot 4$ and $0 \cdot 8$.

The 'long' splitter-plate régime has been investigated in some detail by Roshko[24, 27] in low-speed tests on bluff sections. It was demonstrated that a universal Strouhal number, S^*, could be formed:

$$S^* = \frac{nd}{u_s}$$

where d is the asymptotic wake thickness, derived from free-streamline theory (*see* Section 5.4 above), appropriate to the measured base pressure, and u_s is the velocity on the free streamline at separation, given by

$$u_s = u_\infty(1 - C_{pb})^{1/2},$$

in incompressible flow. The value of S^* was found to be roughly constant at a value of $0 \cdot 16$. If d is identified with the measured wake thickness h', (in fact it is probably proportional to h', approximately), this result would be represented in Fig. 44 by the curve

$$S' = S^*(1 - C_{pb})^{1/2}.$$

It is seen that the results for the 'long' splitter plates correlate well with Roshko's curve although there appears to be some effect of Mach number.

Any interpretation of the results for the 'short' splitter plates must, at this stage, be extremely tentative. Nevertheless, some justification for the positive slope of the curves in Fig. 44 can be obtained from crude theoretical arguments. It will be recalled[3] that the periodic base flow can be represented roughly by the Heisenberg-Roshko flow model, which attempts to match the appropriate free-streamline flow to the Kármán vortex street. The drag which can be supported by a Kármán vortex street is given by

$$C_D = \frac{b}{h}\left\{5 \cdot 66\,\frac{u_v}{u_\infty} - 2 \cdot 24\left(\frac{u_v}{u_\infty}\right)^2\right\}, \tag{1}$$

where b is the distance between the rows of vortices, u_v is the velocity of progression of the street relative to the free stream, and C_D is the drag coefficient based on the trailing-edge thickness. The velocity u_v is related to the shedding frequency n and the wavelength of the vortex street, a, by

$$n = \frac{u_\infty - u_v}{a}$$

or

$$\frac{u_v}{u_\infty} = 1 - \frac{na}{u_\infty}.$$

But $a = 3 \cdot 54b$, and if b is identified with the measured wake thickness h', (again a tentative assumption), we can write

$$\frac{u_v}{u_\infty} = 1 - 3 \cdot 54S'. \tag{2}$$

Now Eppler[44] has shown that within the framework of 'parallel' free-streamline theory the form drag of a section and the base pressure are related by

$$C_D = - C_{pb} \frac{d}{h} \tag{3}$$

where d is the asymptotic distance between the free streamlines. If as before we equate d to h', equations (1), (2) and (3) give a relation between C_{pb} and S' in the form

$$C_{pb} = 28 \cdot 4 S'^2 + 4 \cdot 2 S' - 3 \cdot 42 . \tag{4}$$

It is seen from Fig. 44 that this expression represents to some extent the measured variation of wake Strouhal number with base pressure, for the 'short' splitter-plate range.

6. *Results for other Base Configurations.*

It was seen in the previous section that the attachment, to the base of the section, of a short splitter plate, of length equal to the trailing-edge thickness, is a convenient method of reducing base drag. In this section a report is made of two short tests to measure the base pressure on the model fitted with alternative base configurations, the half-round base and the cavity base (Fig. 7).

6.1. *The Half-Round Base.*

It was shown by Sargent[45] in tests on aerofoil sections with a small degree of trailing-edge bluntness (3% of the chord), that the provision of a rounded, as distinct from a square, trailing edge resulted in a significant saving in drag through the subsonic speed range. In turbo-machinery the blade size is often too small for a sharp trailing edge to be realised and it is current practice to aim at a carefully rounded trailing-edge profile.

On a relatively thick trailing-edge section such as the present model, however, the advantages of rounding the trailing edge are found to be dubious. The afterbody of the basic model was modified by the addition of a semi-circular cylindrical section as in Fig. 7. The variation of the measured pressure on the centre-line of the base with Mach number is illustrated in Fig. 45. Over a small range of Mach number around $0 \cdot 4$ the base pressure is substantially higher than that measured on the basic section, indicating a reduction in overall drag. The schlieren photograph (Fig. 46a) shows that in this condition the point of vortex formation has been displaced downstream, leaving a larger dead-air region than was observed behind the basic section (Fig. 14a). Thus the rounded base is operating in much the same way as a short splitter plate.

At a slightly higher Mach number, however, a change takes place in the base flow pattern and the base pressure falls to a very low value (Fig. 45). At $M_\infty = 0 \cdot 925$, for example, the measured base pressure coefficient was as low as $-1 \cdot 10$. The schlieren photograph (Fig. 46b) taken at a Mach number of $0 \cdot 8$ indicates that, in contrast to the case at lower speeds, there is no 'dead-air region' behind the trailing edge. This might be interpreted as suggesting that the flow is adhered to the base, but in an unsteady condition. Thus it would seem that the provision of a rounded base has presented an opportunity for the vortex street to form very close to the section, exposing the base to the low pressures developed in the 'trough' (*see* Section 3.7 above). This suggestion is supported by the fact that the measured pressures on the base correlate approximately with the peak suction recorded in the wake behind the basic model (Fig. 45). It is significant to note that in the tests by Sargent[45] the model with the largest trailing-edge radius (2% of the chord), displayed a similar, but less pronounced, abrupt increase in overall drag at a Mach number of about $0 \cdot 5$.

There would seem to be a need for tests to investigate the conditions which provoke the change from the more favourable to the distinctly unfavourable base flow pattern. The important point which emerges at this stage, however, is that on sections with a significant degree of trailing-edge thickness, 4% and greater, rounding the trailing edge is not necessarily advantageous from the point of view of drag. While it would appear to be beneficial to delay the separation of the flow by afterbody contouring, with a view to reducing the thickness of the wake, if the flow attachment is unsteady it will have anything but this effect. The danger of the separation points moving in sympathy with the vortex formation draws attention to the importance of incorporating sharp corners at the trailing edge.

6.2. *The Trailing-Edge Cavity.*

The test on the model with a trailing-edge cavity (Fig. 7), was of a somewhat *ad hoc* nature, but the results may serve to emphasise the need for further study of cavities in relation to aerofoil design. According to the steady-base-flow model there is no mechanism by which the existence of a cavity at the base could influence the base pressure. Thus at supersonic speeds the measured base pressures correlate precisely with those measured on the basic section (Fig. 47). At subsonic speeds, however, the base-pressure coefficient for the cavity base is found to be approximately 20% higher. It should be noted that no attempt was made to achieve an optimum cavity size or shape.

In order to interpret this result it is necessary to recall some of the work which has been carried out in recent years on the use of cavities as a means of separation control. The observation of certain natural phenomena, such as the snow-cornice effect[15], has inspired a study of the extent to which cavities in a solid boundary can be used to generate a trapped vortex. If this can be achieved it is known that a flow can be made to negotiate a fairly abrupt pressure rise without incurring significant penalties. In this context examples have been given to show the application of the principle to wind-tunnel diffusers and aerofoil sections[47]. In the case of aerofoils a cavity has usually been incorporated into the upper or lower surface close to the trailing edge. By the application of suction through a slot in the cavity, a standing eddy can be formed and the drag of the section reduced to a very low value. Tests by Hazen *et al*[46] have indicated that the use of suction to establish a trapped eddy does not necessarily result in a nett reduction in drag since the required suction quantities are large and represent a considerable equivalent drag penalty. Nevertheless, the measured drag coefficient of the section tested in Ref. 46 at zero incidence was only 0·013 in the *absence* of suction. This is quite remarkable since the thickness of the aerofoil at the position of the cusp was as great as 8% of the chord.

It would appear that the provision of a rear cavity in a blunt-trailing-edge section, while not necessarily trapping a stable eddy, can still lead to a substantial reduction in the base drag. This decrease in drag can be regarded as an improvement of the wake stability resulting in a decrease in the strength of the vortex street. In such cases where no suction is applied it would appear that if a steady wake flow is achieved, the flow in the neighbourhood of the cavity would resemble more closely the steady base flow behind a step with the slowly circulating eddy, than that generated by a standing 'vortex' as discussed by Ringleb[15], for example. Even in cases where strong suction is applied it is not clear whether the vortex model or the separation/reattachment model of the flow is most valid, and many features of the observations reported in Refs. 46 and 47 can be explained at least qualitatively in terms of the theory of Ref. 10.

In any case a recirculating vortical flow is called for in a steady base flow and the concept of the stability of this 'standing eddy' may provide further enlightenment as to the failure of the rounded base. In the cases where separation takes place from a curved surface, as in the half-round base, the possibility of stable eddies forming in the base flow would appear, intuitively, to be more remote than in cases where separation is provoked at a sharp corner. Thus from these arguments the base flow behind a section with a rounded base could be expected to be less stable, and develop a larger base drag than a section with sharp corners at the rear, and in certain circumstances this is seen to be borne out by observation.

The arguments, concerning wake stability and the advantages to be derived from providing 'protection' for the standing eddies required for a steady base flow, can also be invoked to interpret the effect of a splitter plate (Section 5 above). It would seem that the provision of a solid surface between the eddies would assist stability in a similar way to solid boundaries (the sides of the cavity) encasing them. In this context, however, the progression from 'short' to 'long' splitter plates would need to be accommodated in the arguments as a deterioration of the stabilising mechanism. Thus considerably more thought must be given to this explanation before any definite conclusion can be drawn.

7. *Concluding Remarks.*

The base flow behind a blunt-trailing-edge aerofoil section is characterised by the existence of two flow régimes.

7.1. At subsonic speeds the wake is observed to break up into discrete eddies, which are shed at a well-defined frequency, even under conditions where turbulent flow exists in the boundary layers ahead of separation. The existence of the vortex street appears to be responsible for a low pressure on the base which represents a large drag increment. In normal circumstances, the base drag of sections with a severe degree of trailing-edge thickness is substantially higher than can be accounted for on the basis of steady-flow considerations. The strength of the vortex street, and hence the base pressure, appears to be sensitive to the geometry of the section. This explains why it is difficult to derive a satisfactory correlation of base pressures in terms of simple parameters involving, say, the trailing-edge thickness, or the thickness of the boundary layers approaching the base.

In the context of section geometry, the base configuration itself is observed to have a significant effect on the base pressure. Such arrangements as trailing-edge cavities and splitter plates which in general have little effect in the steady base flow, are found to be beneficial in increasing the base pressure in the unsteady-flow régime. A rear cavity in the section is believed to achieve a reduction in drag by virtue of its stabilising effect on the standing eddies, which must be present as a feature of the steady base flow, but which are normally formed in an unstable fashion and pass downstream into the vortex street.

A splitter plate, a thin two-dimensional flat plate placed in the plane of symmetry of the wake, is also observed to have a powerful effect in reducing the base drag, and it is possible that this can again be attributed to a stabilising action. The base pressure does not rise monotonically with the length of the splitter plate, but was found in the present test, to reach a local maximum when the length of the plate was approximately equal to the trailing-edge thickness. When the length of the splitter plate was increased above twice the trailing-edge thickness the base pressure began to rise again, finally approaching the value appropriate to steady base flow. A number of differences in the flow characteristics were observed as the length of the splitter plate was increased from one to two times the trailing-edge thickness.

On the evidence of tests made on sections with a small degree of trailing-edge bluntness it has sometimes been asserted that rounding the trailing edge results in a reduction of base drag. However, it would appear that if the trailing-edge radius is large a condition can be reached with increasing Mach number (or possibly Reynolds number), when an unsteady attached flow can be generated round the base, and the base drag may rise to a substantially higher value than occurs on a section with a square trailing edge. Thus in the case of sections with a severe degree of trailing-edge thickness, if afterbody contouring is envisaged, and this may well be beneficial, it would seem wise to incorporate sharp corners to fix the separation points.

7.2. As the Mach number approaches unity the periodic effects collapse and subsequently the base flow closely resembles the ideal steady base flow discussed in the theory. However, this is not observed to be accompanied by a significant rise in the base pressure since the steady base flow itself exhibits an abrupt fall in the base pressure at transonic speeds (*see* Section 7.3 below). [In the case of sections with a small degree of trailing-edge thickness the second effect more than off-sets the first and the base drag increases rapidly near sonic speed.]

7.3. The base pressure on a rearward-facing step at subsonic speeds is high, compared with that on a blunt-trailing-edge aerofoil section under nominally equivalent conditions. The base-pressure coefficient measured in the present test lay in the region of $-0 \cdot 2$. No evidence of periodic effects in the base flow behind the step could be detected.

With increasing Mach number, as soon as local supersonic flow is established at the step, the base pressure undergoes an abrupt decrease. This effect can be traced to the modification of the pressure distribution through the reattachment region on the downstream surface. At subsonic speeds there is observed to be an overall decrease in static pressure downstream of the reattachment point, the pressure finally approaching ambient static pressure. In the case of the supersonic reattaching flow, however, a substantial pressure recovery takes place downstream of reattachment. The pressure rise from the base pressure to that at the reattachment point is determined by conditions in the free shear layer and is to some extent insensitive to the base pressure. The final recovery pressure far downstream is close to the free-stream static pressure and can be regarded as a fixed quantity. Thus the base pressure depends ultimately on the pressure recovery achieved from the reattachment point onwards, and with a sharp increase in this pressure recovery at transonic speeds the base pressure is forced to decrease.

It was shown in Ref. 10 that this effect can be accounted for quantitatively on the basis of steady-flow theory once the correct reattachment conditions are taken into consideration.

Acknowledgement.

The authors are indebted to Mr. H. H. Pearcey for useful criticism of this paper.

The model used in the tests was constructed by the staff of the Aerodynamics Division aerofoil workshop under the direction of Mr. W. W. Smith.

NOTATION

x, y	Cartesian co-ordinates
c	Chord of basic section
h	Trailing-edge thickness of basic section
α	Incidence
l	Length of splitter plate, length of separated region
M	Mach number
Re	Reynolds number
p	Static pressure
C_p	Pressure coefficient $= \dfrac{p - p_\infty}{\frac{1}{2}\rho_\infty u_\infty^2}$
H	Pitot pressure
ρ	Density
u	Velocity
u^*	Ratio of velocity in boundary layer to that in the external stream
δ	Boundary-layer thickness
C_L	Lift coefficient
n	Vortex-shedding frequency
S	Strouhal number, $= \dfrac{nh}{u_\infty}$
h'	Thickness of wake (defined in Fig. 25)
S'	Strouhal number based on wake thicknesses, $= \dfrac{nh'}{u_\infty}$
N	Recompression parameter.

Subscripts

0	Stagnation conditions
∞	Free-stream conditions
b	Conditions on base
s	Conditions in the external stream after an isentropic expansion from p_∞ to p_b, i.e. $M_s^2 = \dfrac{2}{\gamma - 1}\left[\left(\dfrac{p_\infty}{p_b}\right)^{\gamma-1/\gamma}\left\{1 + \dfrac{\gamma - 1}{2} M_\infty^2\right\} - 1\right]$
r	Conditions at the reattachment point.

REFERENCES

No.	Author(s)	Title, etc.
1	D. R. Chapman and R. H. Kester.	Effect of trailing-edge thickness on lift at supersonic velocities. N.A.C.A. Tech. Note 3504. June, 1955.
2	D. R. Chapman	Reduction of profile drag at supersonic velocities by the use of airfoil sections having a blunt trailing edge. N.A.C.A. Tech. Note 3503. September, 1955.
3	J. F. Nash	A review of research on two-dimensional base flow. A.R.C. R. & M. 3323. March, 1962.
4	E. J. Saltzman	Preliminary base pressures obtained from the X–15 airplane at Mach numbers from 1·1 to 3·2. N.A.S.A. Tech. Note D–1056. August, 1961.
5	J. F. Nash	Unpublished N.P.L. work. 1961.
6	H. H. Pearcey	The design of wing sections for swept wings at transonic speeds. Paper presented at 2nd International Congress of Aeronautical Science, Zürich, Switzerland. 1960. *Advances in Aeronautical Sciences*, Vol. 3, p. 277.
7	D. W. Holder, H. H. Pearcey and J. F. Nash	Some aerodynamic advantages of thick trailing edges in high-speed flight. Paper presented to Royal Aeronautical Society. February, 1962.
8	H. H. Pearcey	Shock-induced separation and its prevention by design and boundary-layer control. Part IV of *Boundary layer and flow control*. Editor G. V. Lachmann. Pergamon Press. 1961.
9	T. H. Moulden, Miss A. G. J. Macdonald and Miss R. L. Warren.	Some tests at transonic speeds on three related cambered aerofoils with thick trailing edges. Unpublished N.P.L. work.
10	J. F. Nash	An analysis of two-dimensional turbulent base flow, including the effect of the approaching boundary layer. A.R.C. R. & M. 3344. July, 1962.
11	S. Goldstein (Editor)	*Modern developments in fluid dynamics.* Clarendon Press, Oxford, 1938.
12	A. Roshko	Experiments on the flow past a circular cylinder at very high Reynolds number. *J. Fluid Mech.*, Vol. 10, Part 3, p. 345. May, 1961.
13	S. F. Hoerner	*Fluid-dynamic drag.* Published by the author. 1958.
14	H. Thomann	Measurements of the recovery temperature in the wake of a cylinder and of a wedge at Mach numbers between 0·5 and 3. F.F.A. Report 84, Sweden. June, 1959.

No.	*Author(s)*	*Title, etc.*
15	F. O. Ringleb	Separation control by trapped vortices. Chapter in Part II of *Boundary layer and flow control.* Editor G. V. Lachmann. Pergamon Press. 1961.
16	I. M. Hall	The operation of the N.P.L. 18 in. × 14 in. wind tunnel in the transonic speed range. A.R.C. C.P. 338. January, 1957.
17	H. H. Pearcey, C. S. Sinnott and J. Osborne.	Some effects of wind tunnel interference observed in tests on two-dimensional aerofoils at subsonic and transonic speeds. AGARD Report 296. March, 1959.
18	D. W. Holder, R. J. North and G. P. Wood.	Optical methods for examining the flow in high speed wind tunnel. AGARDograph 23. November, 1956.
19	T. H. Moulden	Unpublished N.P.L. work.
20	D. R. Chapman	An analysis of base pressure at supersonic velocities and comparison with experiment. N.A.C.A. Tech. Note 2137. July, 1950.
21	G. E. Gadd, D. W. Holder and J. D. Regan.	Base pressure in supersonic flow. A.R.C. C.P. 271. March, 1955.
22	H. H. Korst	A theory for base pressures in transonic and supersonic flow. *J. App. Mech.*, Vol. 23, No. 4, p. 593. December, 1956.
23	J. W. Cleary and G. L. Stevens	The effects at transonic speeds of thickening the trailing edge of a wing with a 4 per cent-thick circular-arc airfoil. N.A.C.A. Research Memo. A51J11. December, 1951.
24	A. Roshko	On the drag and shedding frequency of two-dimensional bluff bodies. N.A.C.A. Tech. Note 3169. July, 1954.
25	G. E. Gadd	Two-dimensional separated or cavitating flow past a flat plate normal to the stream. A.R.C. C.P. 697. November, 1962.
26	R. Fail, J. A. Lawford and R. C. W. Eyre.	Low speed experiments on the wake characteristics of flat plates normal to an airstream. A.R.C. R. & M. 3120. June, 1957.
27	A. Roshko	On the wake and drag of bluff bodies. *J. Ae. Sci.*, Vol. 22, p. 124. February, 1955.
28	A. Fage and F. C. Johansen ..	The structure of vortex sheets. A.R.C. R. & M. 1143. August, 1927.
29	I. Tani, M. Iuchi and H. Komoda.	Experimental investigation of flow separation associated with a step or a groove. Aero. Res. Inst., University of Tokyo, Report 364 (Vol. 27, No. 4). April, 1961.

No.	Author(s)	Title, etc.
30	S. F. Hoerner	Base drag and thick trailing edges. *J.Ae.Sci.*, Vol. 17, p. 622. October, 1950.
31	K. Wieghardt	Erhöhung des turbulenten Reibungswiderstandes durch Oberflächenstörungen. *Forschungshefte für Schiffstechnik*, Heft 2, p. 65. April, 1953. (B.S.R.A. Transl. No. 322.)
32	J. F. Nash	The effect of an initial boundary layer on the development of a turbulent free shear layer. A.R.C. C.P. 682. June, 1962.
33	H. McDonald	Turbulent shear layer reattachment with special emphasis on the base pressure problem. English Electric Aviation Ltd., Warton. Aerodynamics Tech. Note Ae. 175. February, 1963.
34	R. A. Seban and A. M. Levy ..	The effect of a downstream splitter plate on the heat transfer from a circular cylinder normal to an air stream. W.A.D.C. Tech. Report 57–479. A.S.T.I.A. Document Ad 155765. University of California. August, 1957.
35	M. Arie and H. Rouse ..	Experiments on two-dimensional flow over a normal wall. *J. Fluid Mech.*, Vol. 1, Part 2, p. 129. July, 1956.
36	R. C. Pankhurst and B. Thwaites	Experiments on the flow past a porous circular cylinder fitted with a Thwaites flap.
	W. S. Walker	With Appendix: Smoke visualisation of flow past circular cylinder with Thwaites flap. A.R.C. R. & M. 2787. October, 1950.
37	D. A. Spence	The characteristic frequencies of small oscillations in the flow past bluff bodies. R.A.E. Report Aero. 2532. A.R.C. 17 948. May, 1955.
38	Ph. Poisson-Quinton and P. Jousserandot.	Influence du soufflage au voisinage du bord de finite sur les caracteristiques aérodynamique d'une aile aux grandes vitesses. *La Recherche Aéronautique*, No. 56, p. 21. February, 1957.
39	Y. C. Fung	Fluctuating lift and drag acting on a cylinder in a flow at supercritical Reynolds numbers. *J. Aero/Space Sci.*, Vol. 27, p. 801. November, 1960.
40	J. H. Gerrard	An experimental investigation of the oscillating lift and drag of a circular cylinder shedding turbulent vortices. *J. Fluid Mech.*, Vol. 11, Part 2, p. 244. September, 1961.
41	R. A. Shaw	An explanation of vortex shedding on the basis of pulses travelling at the speed of sound. A.R.C. 18 455. May, 1956.

(92363) D

No.	*Author(s)*	*Title, etc.*
42	N. E. Joukowski	I. A modification of Kirchoff's method of determining a two-dimensional motion of a fluid given a constant velocity along an unknown streamline. II. Determination of the motion of a fluid for any condition given on a streamline. *Rec. Math.*, Vol. 25. (Also *Collected works of N. E. Joukowski*, Vol. III, Issue 3, Trans. C.A.H.I., Moscow.)
43	A. Roshko	A new hodograph for free-streamline theory. N.A.C.A. Tech. Note 3168. July, 1954.
44	R. Eppler	Beiträge zu Theorie und Anwendung der unstetigen Strömungen. *J. rat. Mech. Analysis*, Vol. 3, p. 591. 1954.
45	R. F. Sargent	Tests on N.A.C.A. 0012 with various thick trailing edges at high speeds. A.R.C. R. & M. 2209. November, 1942.
46	D. C. Hazen, R. F. Lehnert, T. E. Sweeney and F. O. Ringleb.	Preliminary report on circulation control by means of trailing edge suction and the cusp effect. Princeton University, Aero. Eng. Report 234. June, 1953.
47	C. D. Perkins and D. C. Hazen	Some recent advances in boundary layer and circulation control. Paper presented to Fourth Anglo-American Aeronautical Conference, London. September, 1953.
48	C. Bourque and B. G. Newman	Reattachment of a two-dimensional incompressible jet to an adjacent surface. *Aero. Quart.*, Vol. 11, Part 3, p. 201. August, 1960.
	See also: B. G. Newman ..	The deflection of plane jets by adjacent boundaries—Coanda effect. Chapter in Vol. 1 of *Boundary layer and flow control.* Editor G. V. Lachmann, Pergamon Press. 1961.
49	A. Heyser and F. Maurer ..	Experimentelle Untersuchungen an festen Spoilern und Strahlspoilern bei Machschen Zahlen von 0·6 bis 2·8. *Z. Flugwiss.*, 10, Heft 4/5. April/May, 1962.
50	C. J. Wood	An interim note on two-dimensional base bleed. A.R.C. 24 361. January, 1963.
	See also: C. J. Wood	The effect of base bleed on a periodic wake. *J. R. Ae. S.*, Vol. 68, p. 477. July, 1964.

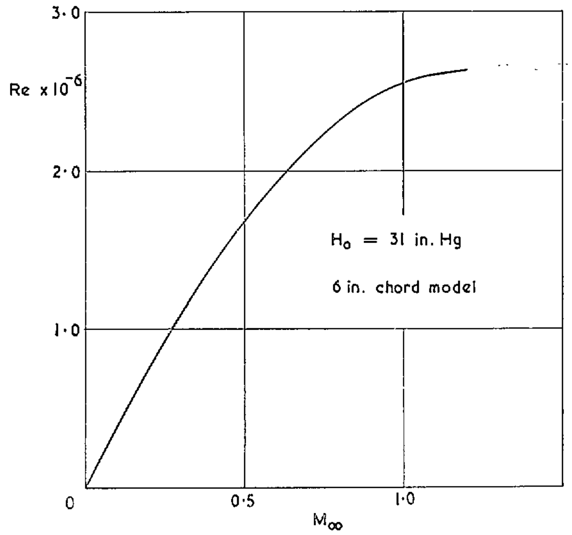

FIG. 1. Increase of chord Reynolds number with Mach number.

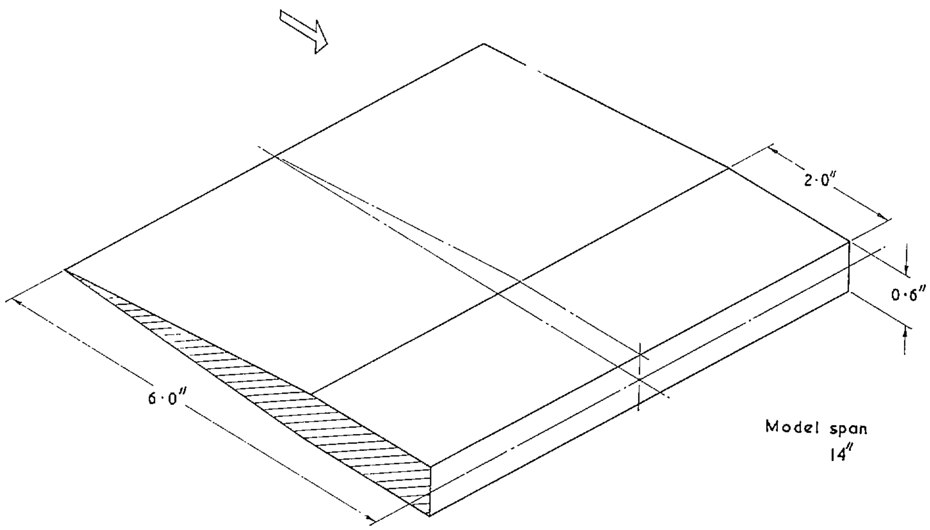

FIG. 2. Diagram of basic model.

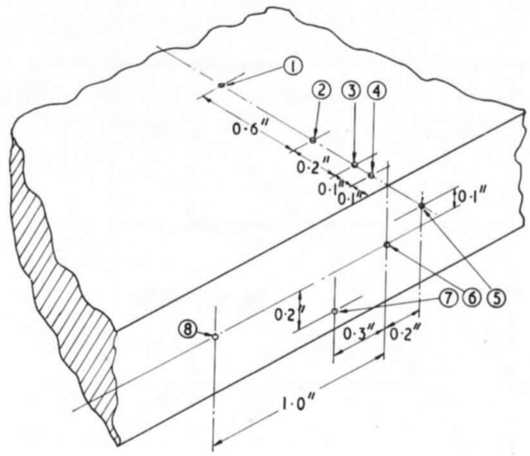

FIG. 3. Location of pressure tappings on base and afterbody.

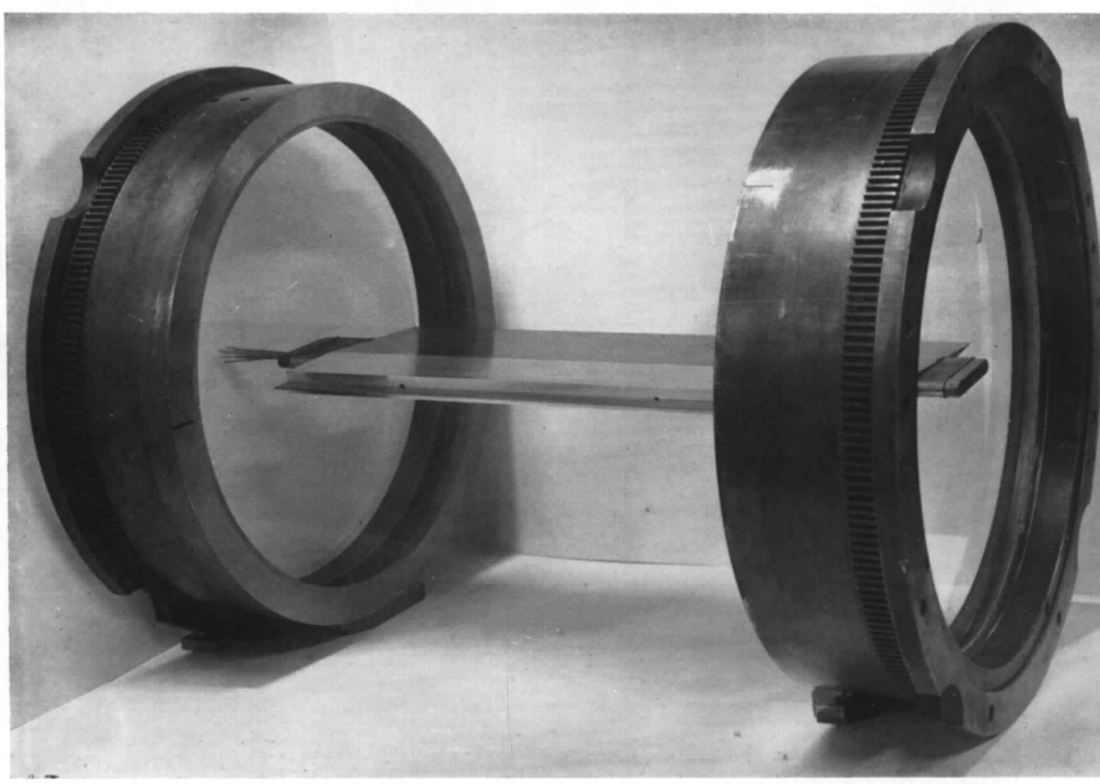

FIG. 4. Model mounted in turn-tables.

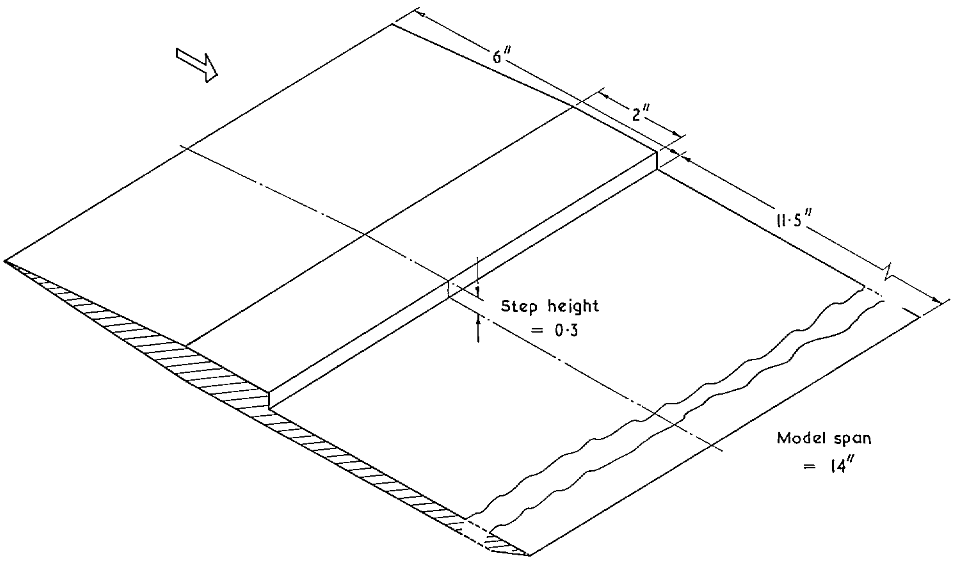

FIG. 5. Diagram of model arranged for backward-facing step.

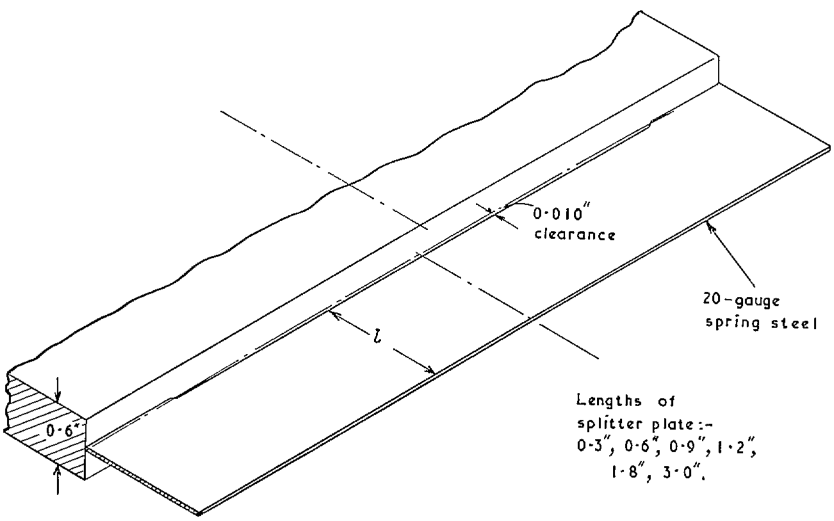

FIG. 6. Diagram of model with splitter plate.

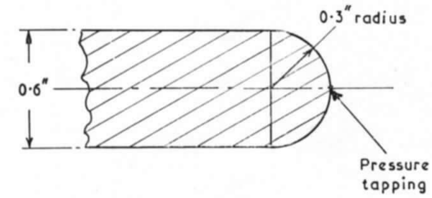

FIG. 7a. Half-round base.

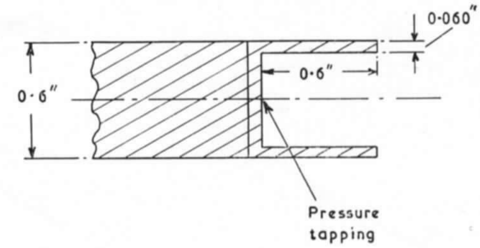

FIG. 7b. Cavity base.

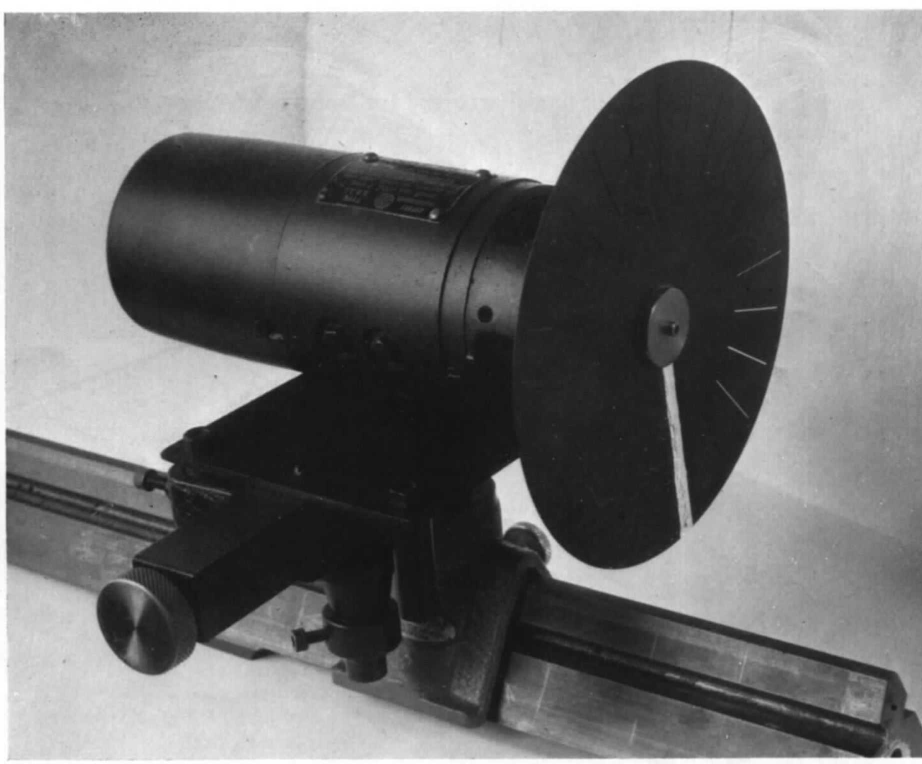

FIG. 8. The stroboscope disc and motor.

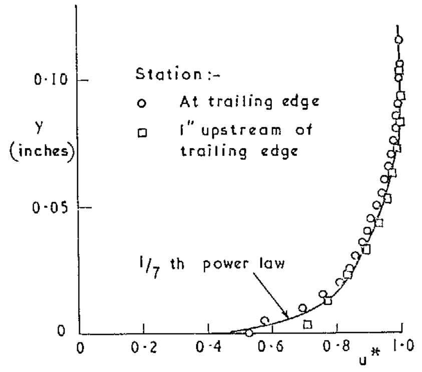

FIG. 9. Boundary-layer profiles on basic model, $M_\infty = 0 \cdot 8$.

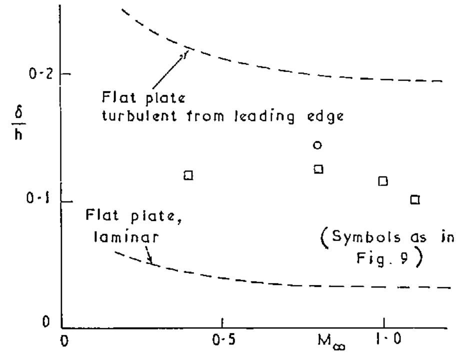

FIG. 10. Variation of boundary-layer thickness with Mach number.

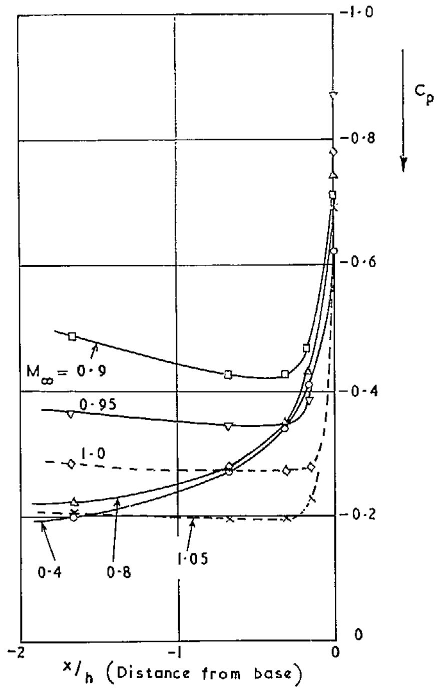

FIG. 11. Pressure distribution on model surface upstream of base.

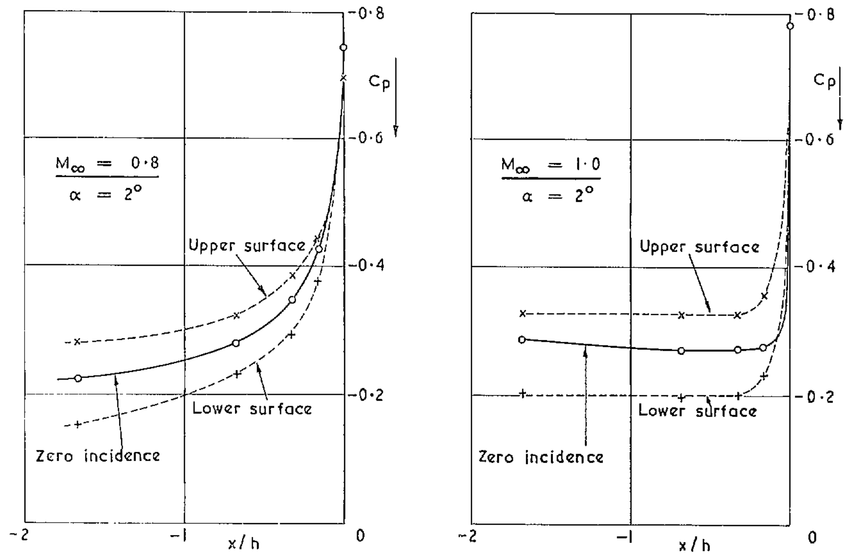

FIG. 12. Effect of incidence on surface pressures upstream of base.

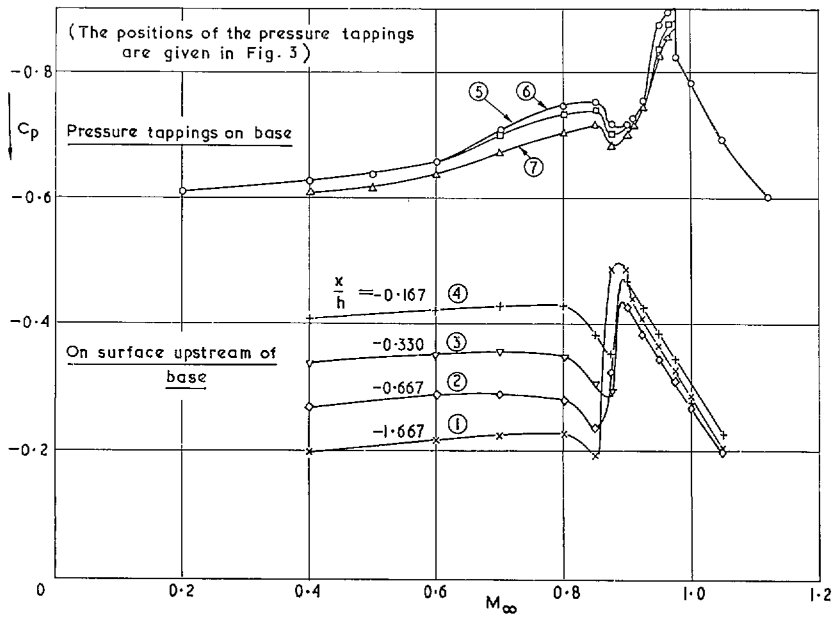

FIG. 13. Pressures on basic model. (Zero incidence.)

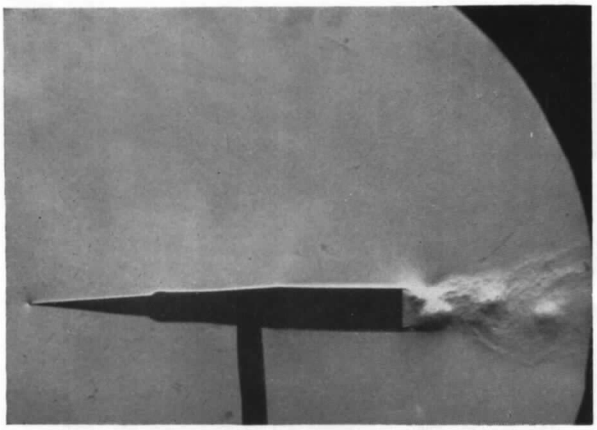

(a) $M_\infty = 0 \cdot 4$.

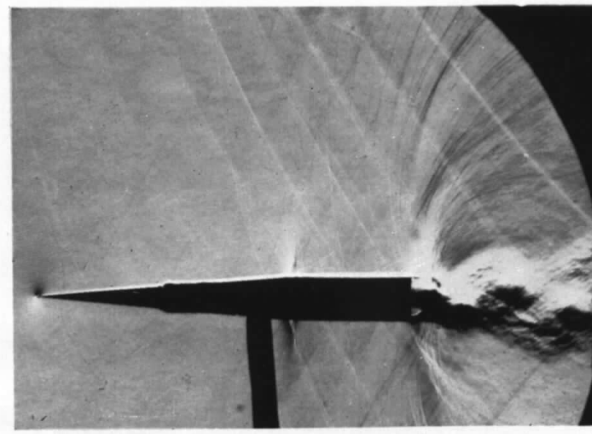

(b) $M_\infty = 0 \cdot 8$.

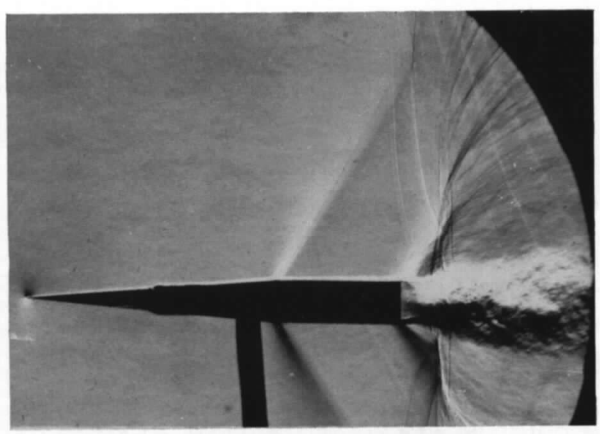

(c) $M_\infty = 0 \cdot 9$

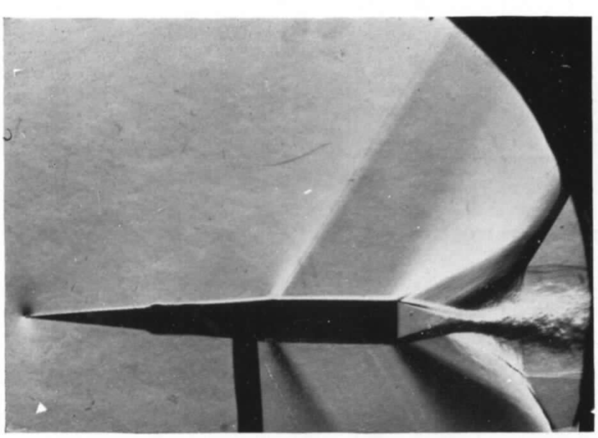

(d) $M_\infty = 1 \cdot 0$.

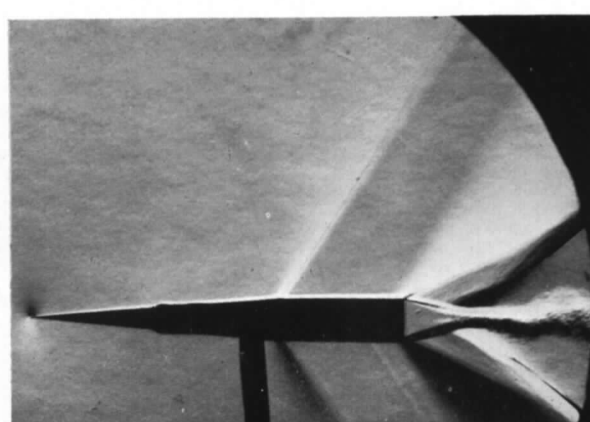

(e) $M_\infty = 1 \cdot 12$.

FIG. 14. Subsonic and transonic flow past a blunt-trailing-edge section.

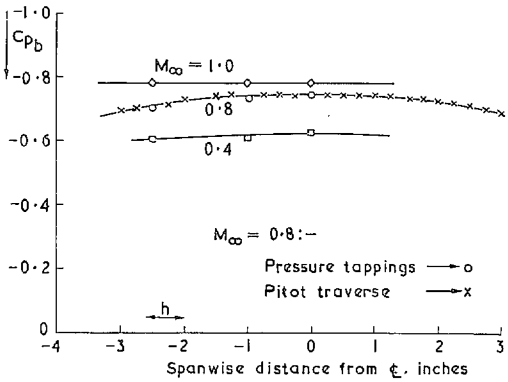

FIG. 15. Spanwise uniformity of base pressure.

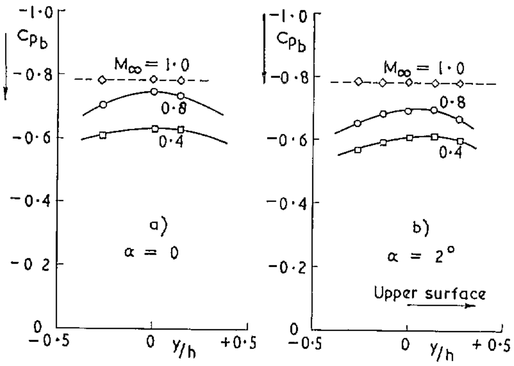

FIG. 16. Variation of pressure across base.

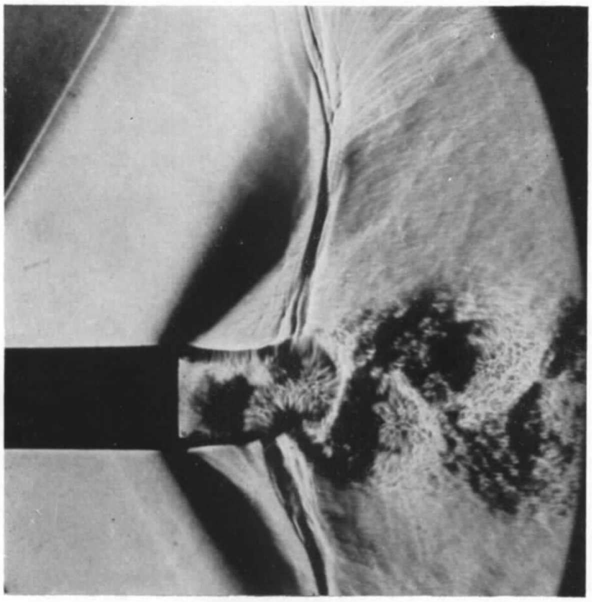

(a) $M_\infty = 0\cdot925$.

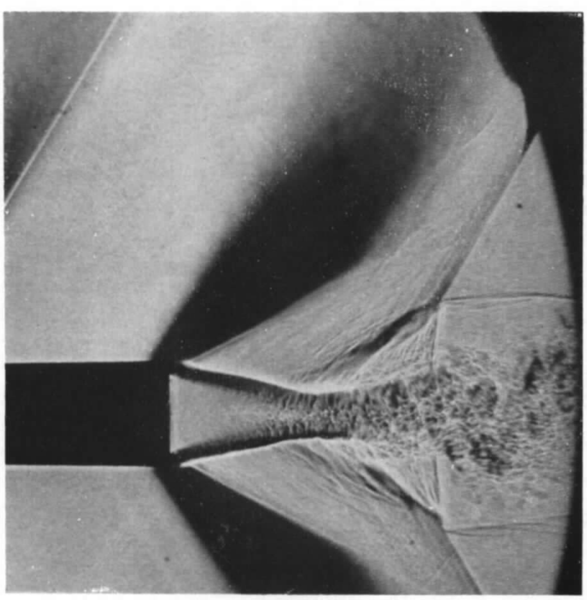

(b) $M_\infty = 1\cdot0$.

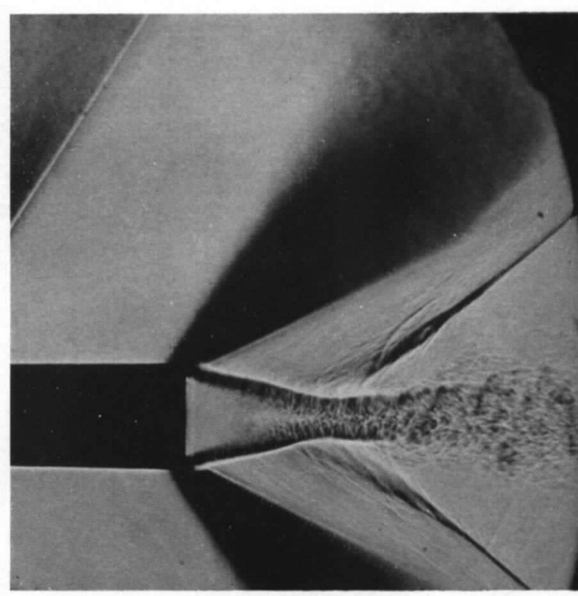

(c) $M_\infty = 1\cdot05$.

FIG. 17. Phases in the base flow behind a blunt-trailing-edge section at transonic speeds.

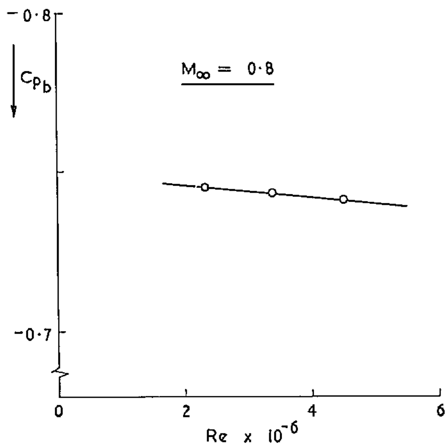

FIG. 18. Effect of Reynolds number on base pressure.

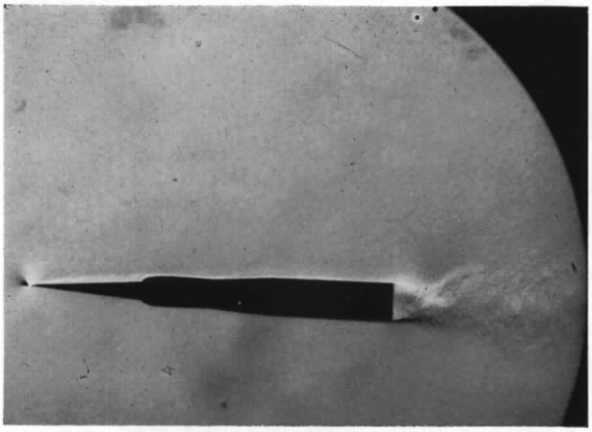

(a) $M_\infty = 0{\cdot}4$.

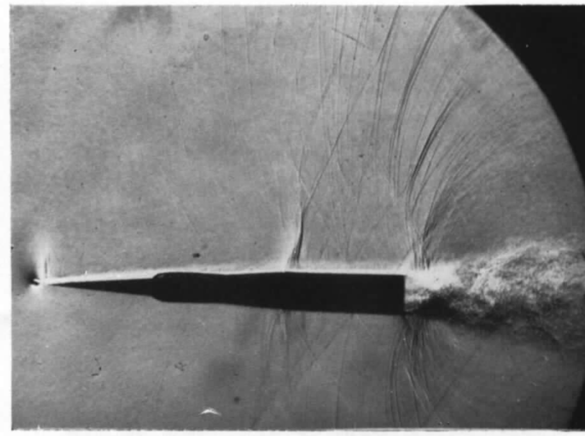

(b) $M_\infty = 0{\cdot}8$.

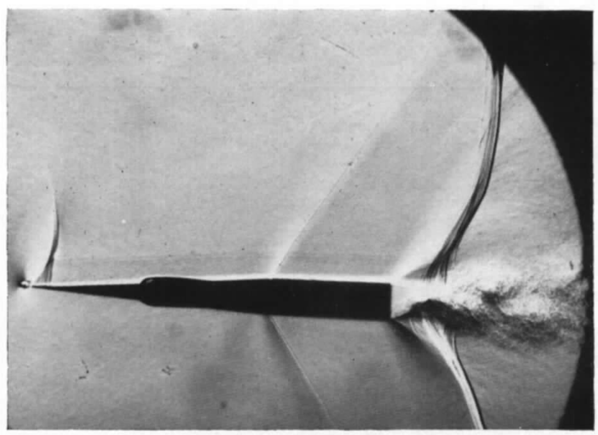

(c) $M_\infty = 0{\cdot}95$.

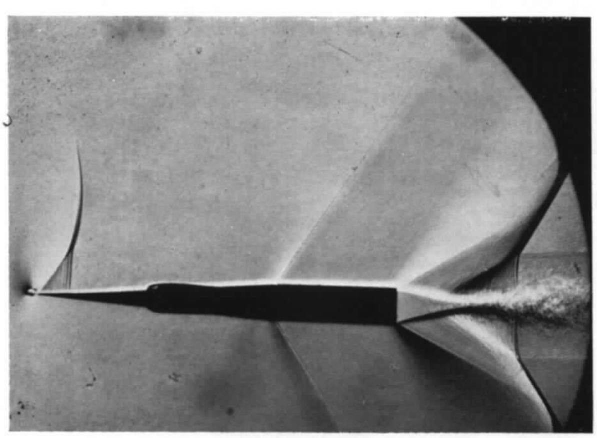

(d) $M_\infty = 1{\cdot}0$.

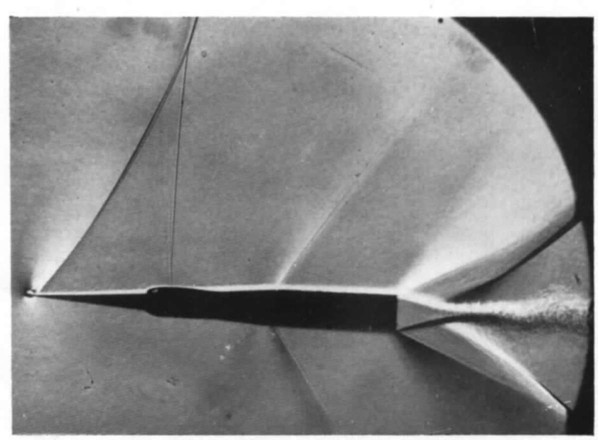

(e) $M_\infty = 1{\cdot}1$.

FIG. 19. The flow past the model at 2° incidence.

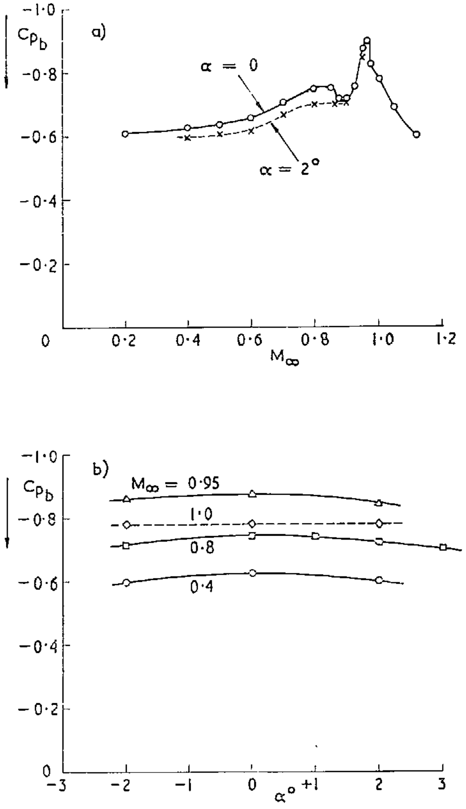

FIG. 20. The effect of incidence on base pressure.

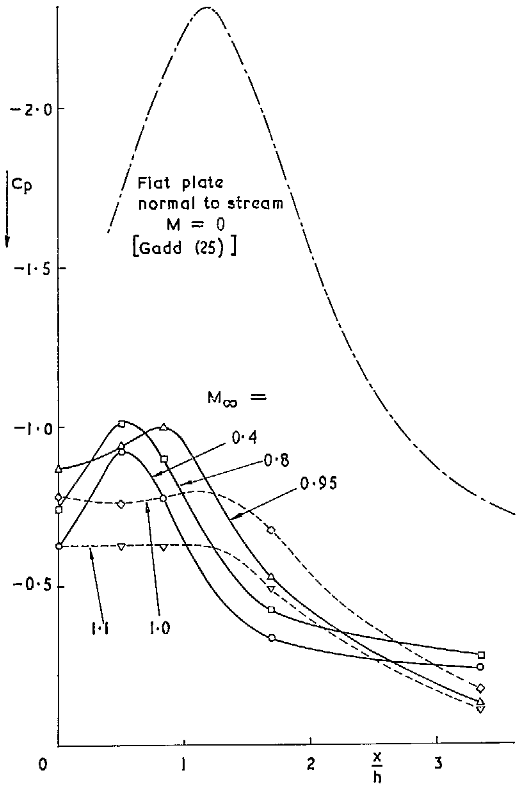

FIG. 21. Static pressure on centre-line of wake.

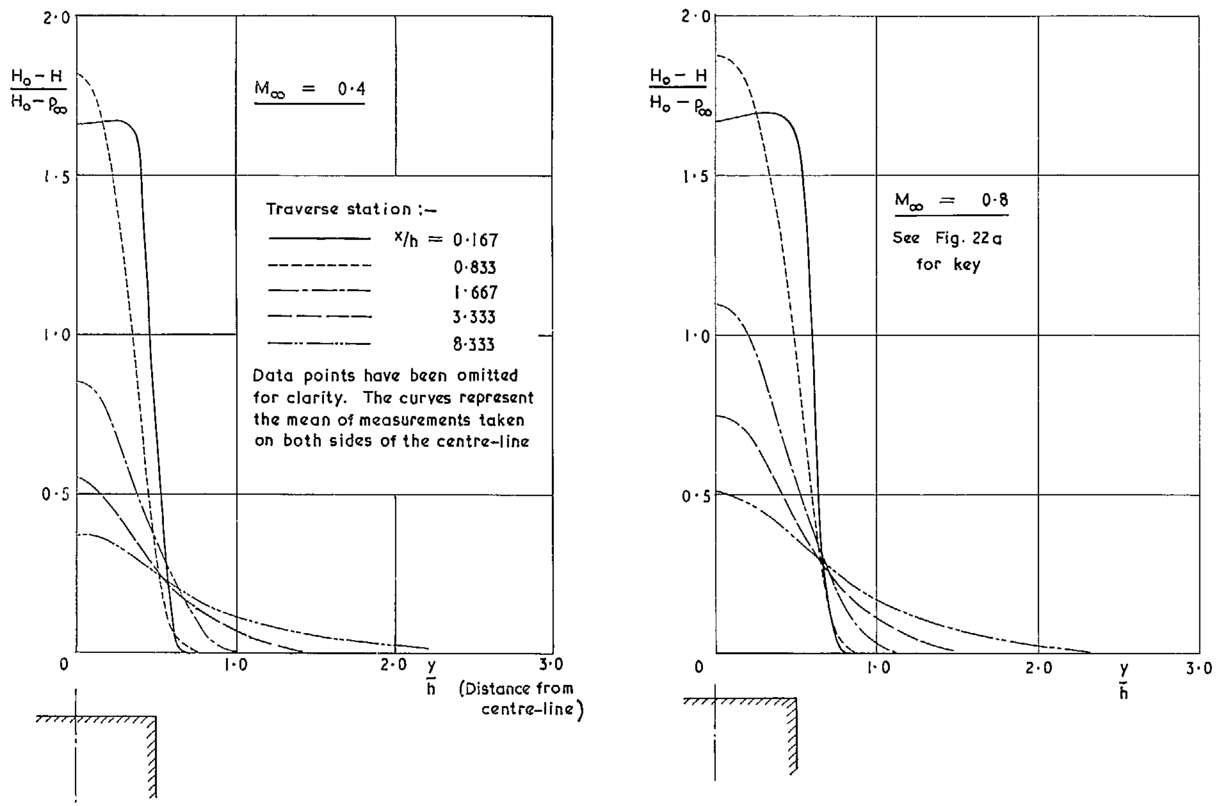

FIGS. 22a and b. Wake exploration. (Pitot pressure.)

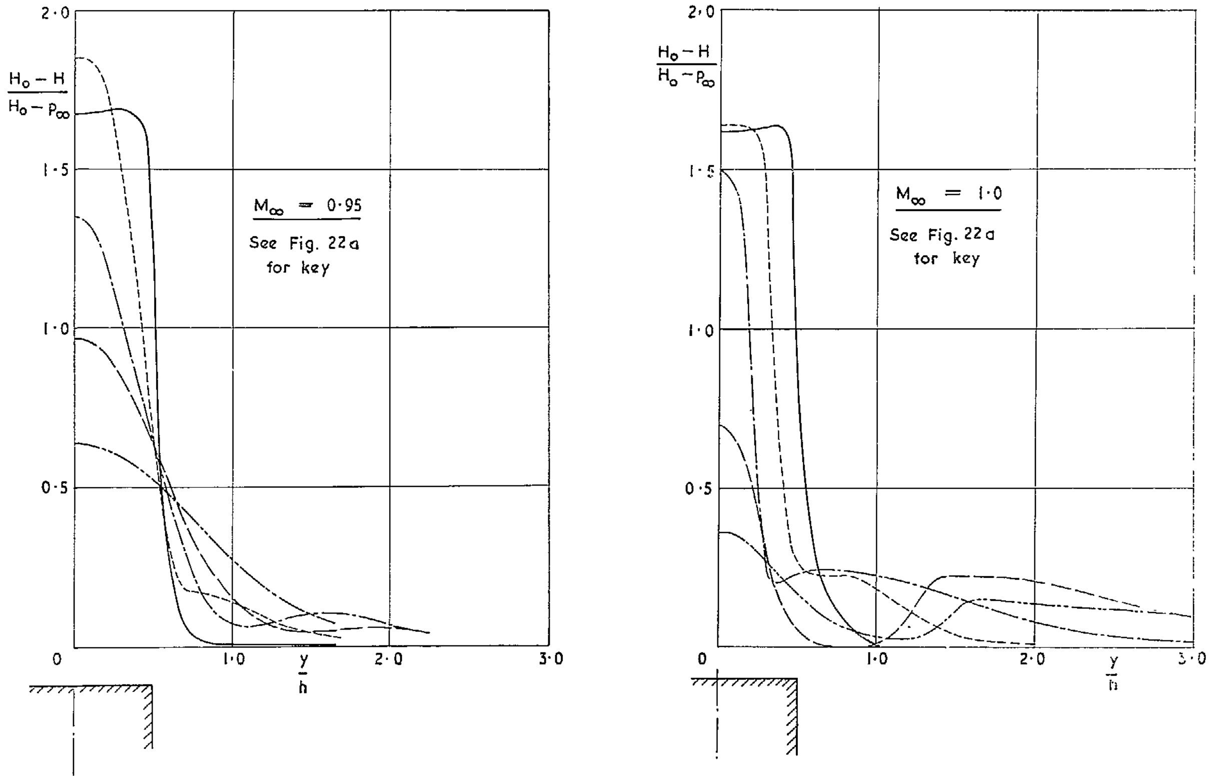

FIGS. 22c and d. Wake exploration. (Pitot pressure.)

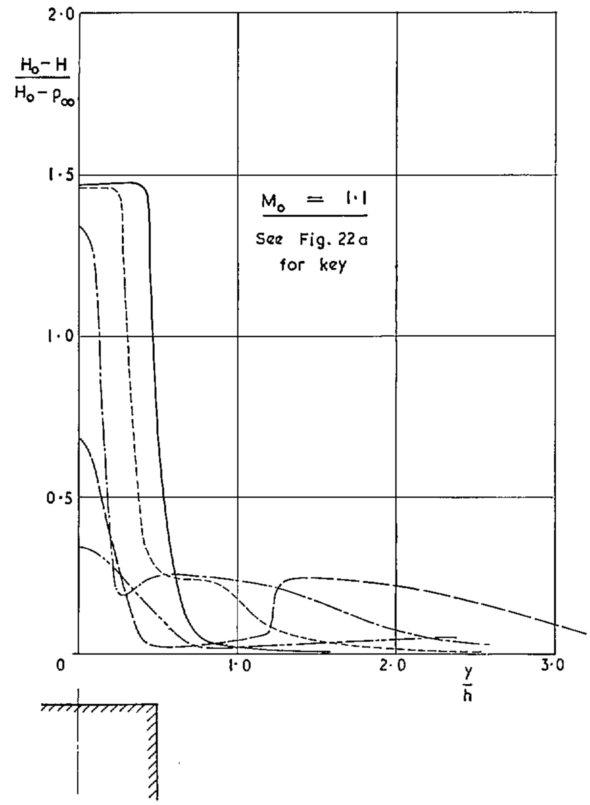

FIG. 22e. Wake exploration. (Pitot pressure.)

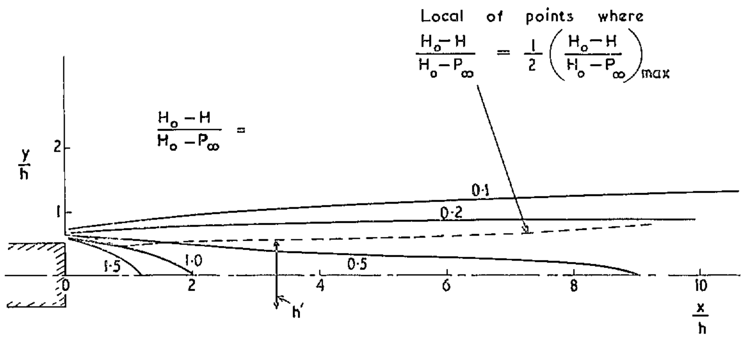

FIG. 23. Pitot pressure contours in wake ($M_\infty = 0 \cdot 8$).

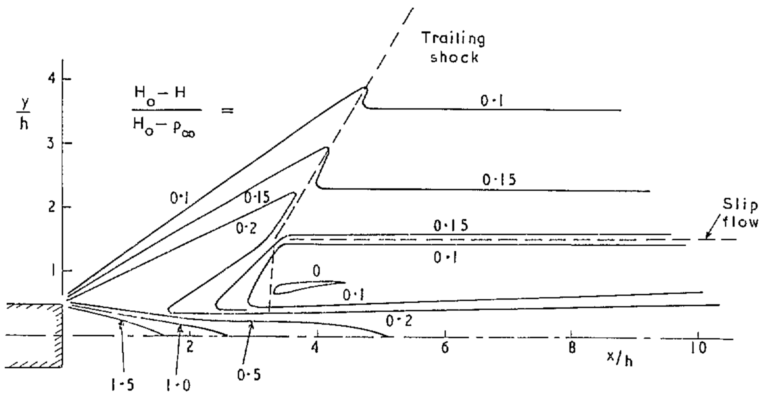

FIG. 24. Pitot pressure contours in wake ($M_\infty = 1 \cdot 0$).

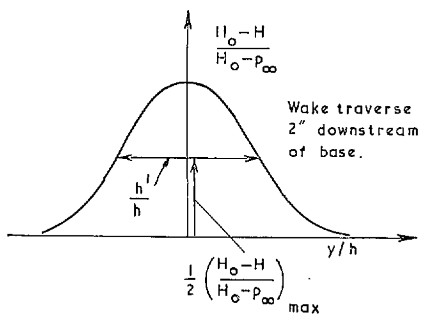

FIG. 25. Definition of h'.

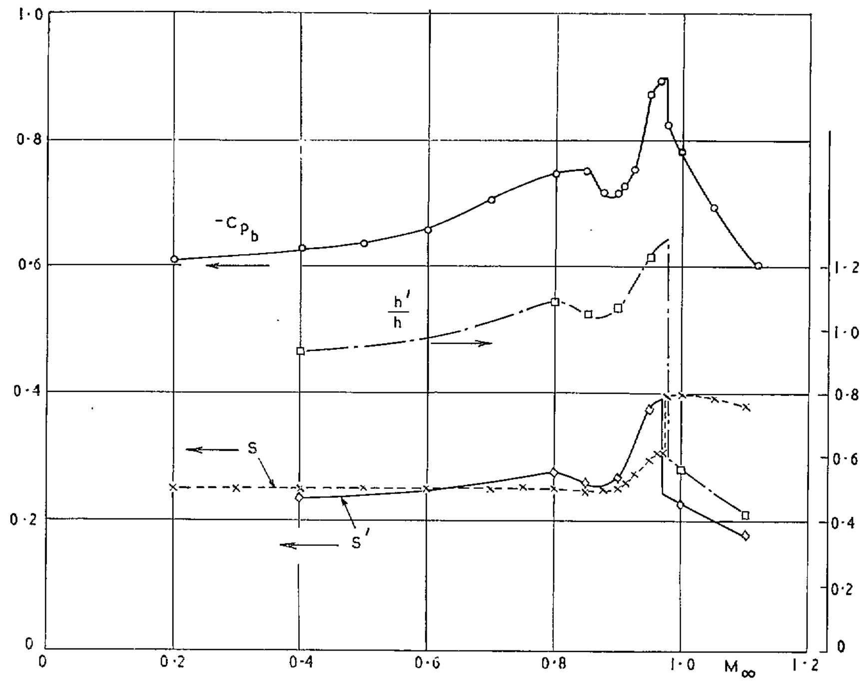

FIG. 26. Relation between base pressure, wake thickness, and vortex-shedding frequency.

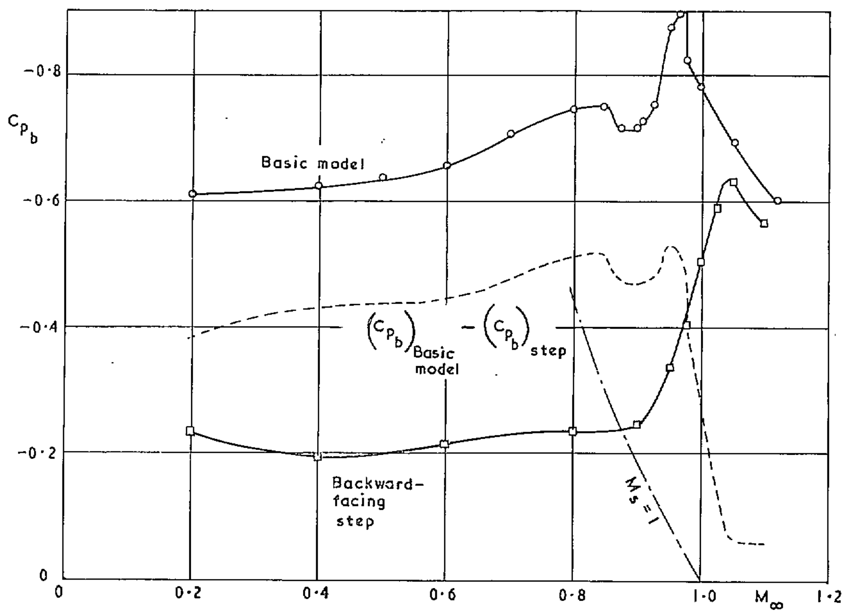

FIG. 27. Base pressure on step.

(92363) F

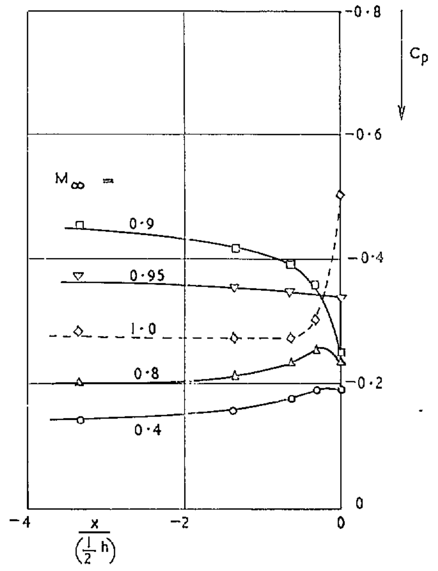

FIG. 28. Pressure distribution on surface upstream of step.

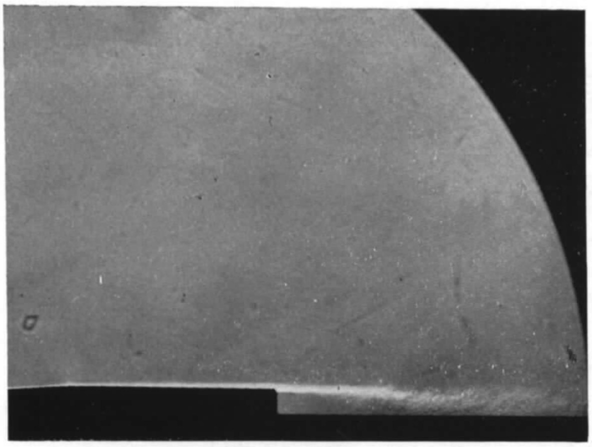

(a) $M_\infty = 0\cdot4$.

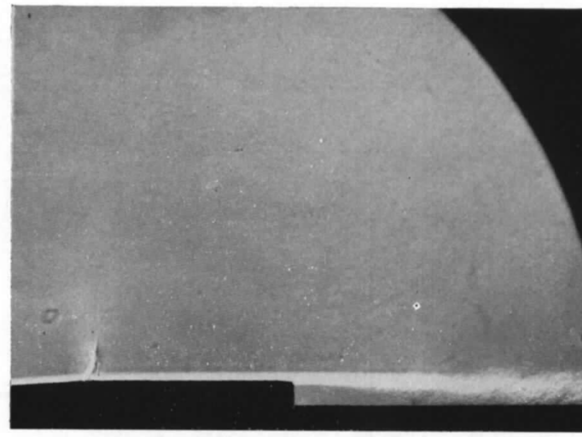

(b) $M_\infty = 0\cdot8$.

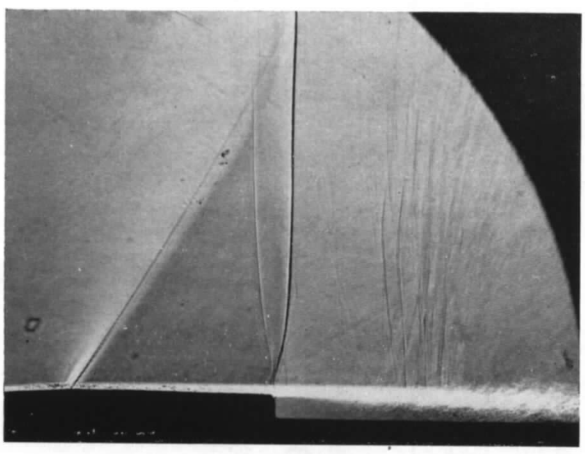

(c) $M_\infty = 0\cdot9$.

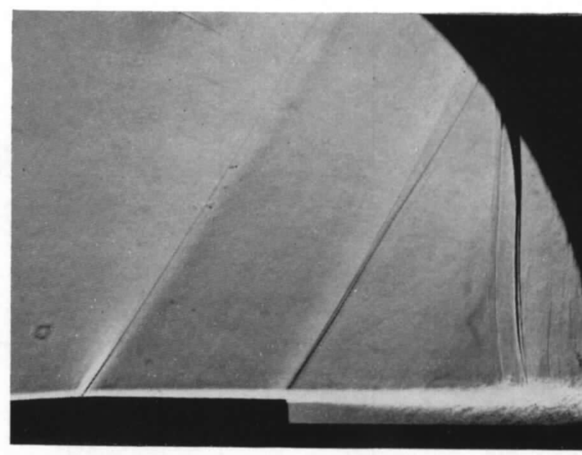

(d) $M_\infty = 0\cdot95$.

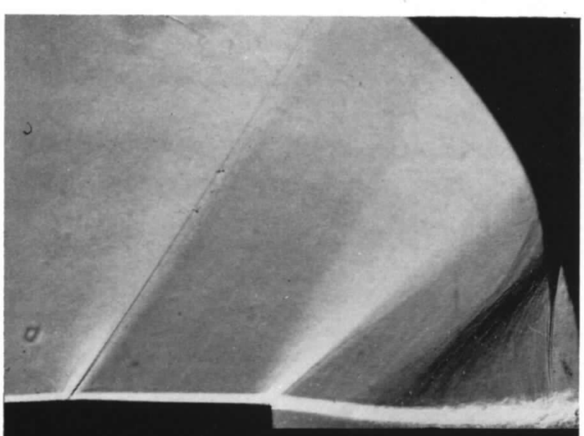

(e) $M_\infty = 1\cdot0$.

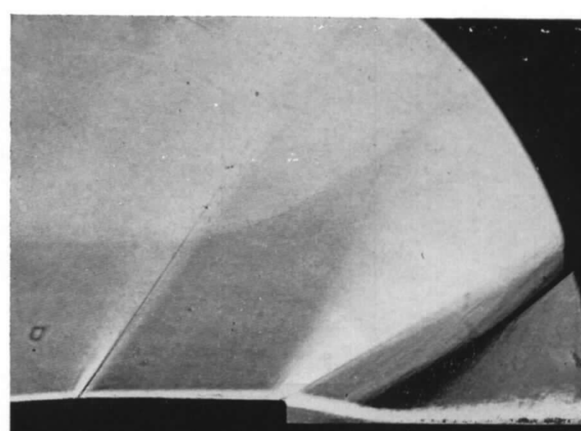

(f) $M_\infty = 1\cdot1$.

FIG. 29. Subsonic and transonic flow past a step.

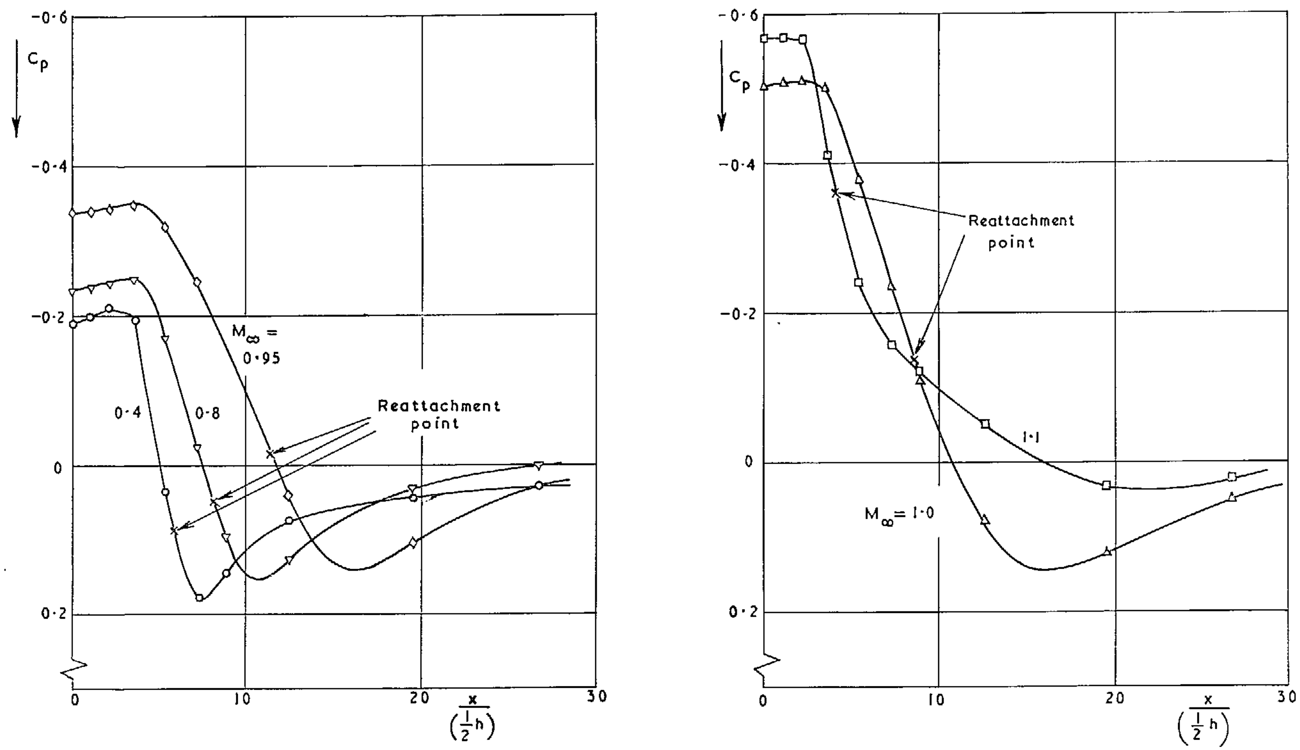

FIGS. 30a and b. Pressure distribution on surface downstream of step.

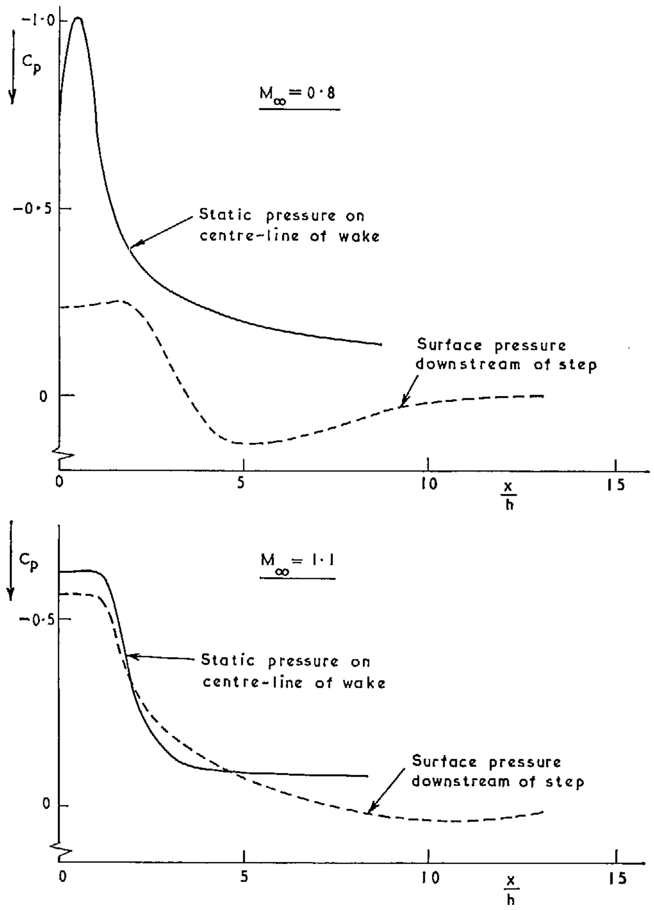

FIG. 31. Comparison between pressure distribution on surface downstream of step and static pressure in wake of basic model.

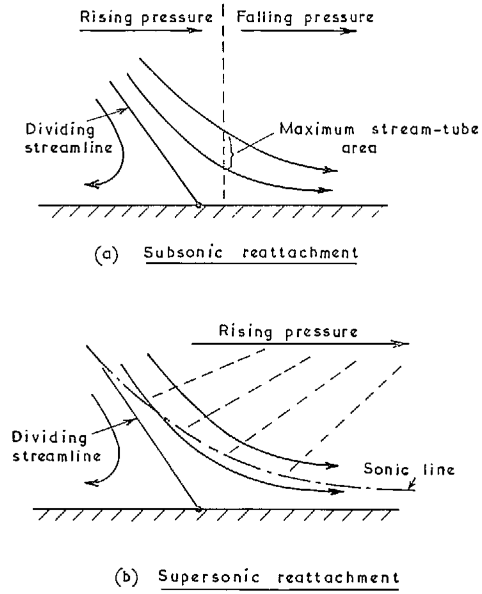

FIG. 32. Streamline patterns in reattachment region (schematic).

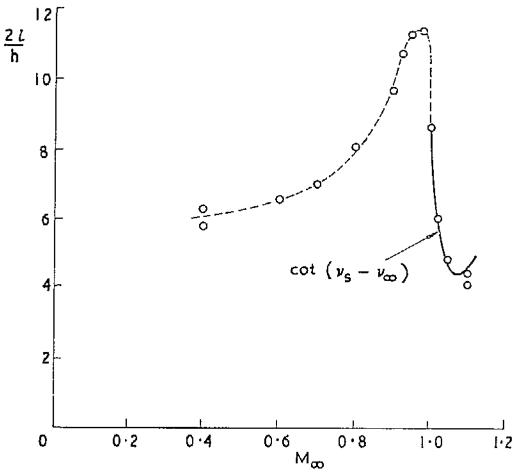

FIG. 33. Length of region of separation. (Distance of reattachment point from step.)

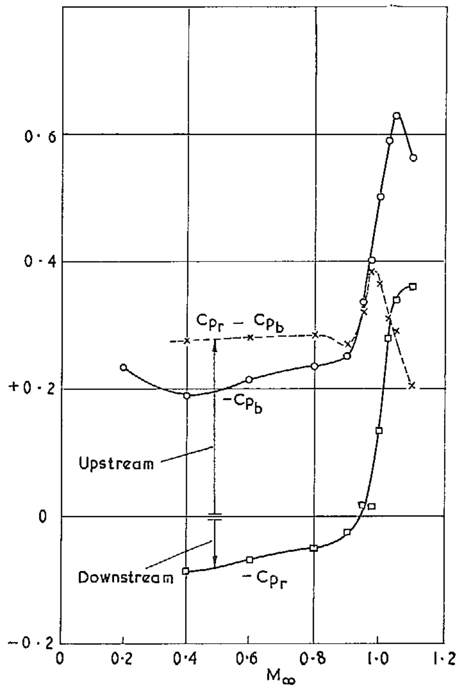

FIG. 34. Pressure recovery before and after reattachment.

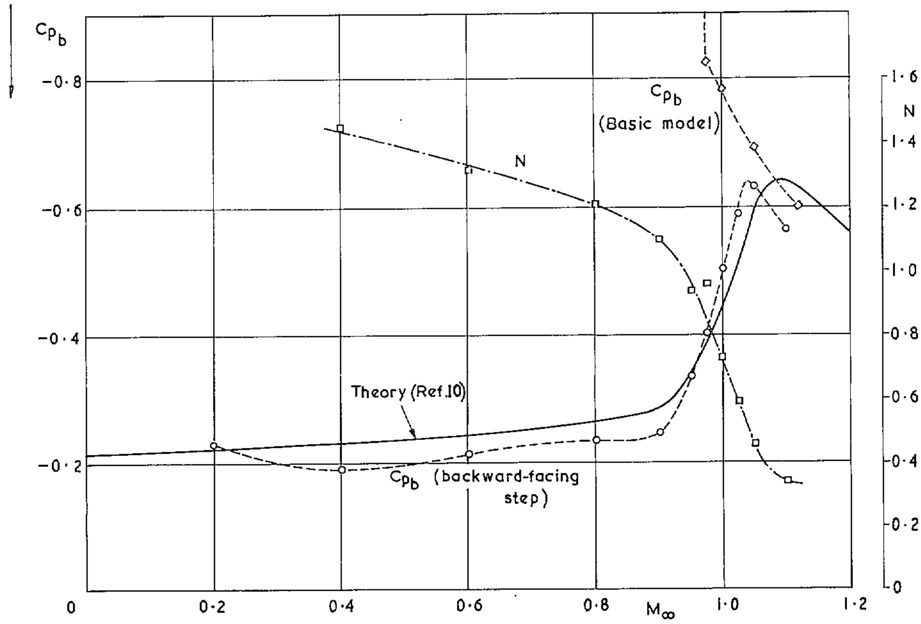

FIG. 35. Relation between base pressure on step and reattachment parameter N.

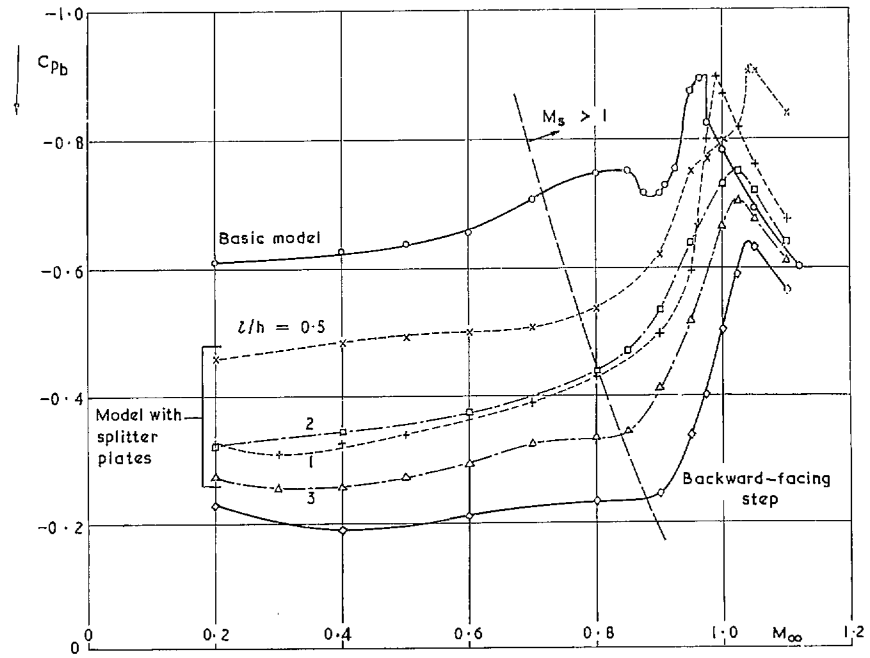

FIG. 36. Base pressure on model with splitter plate.

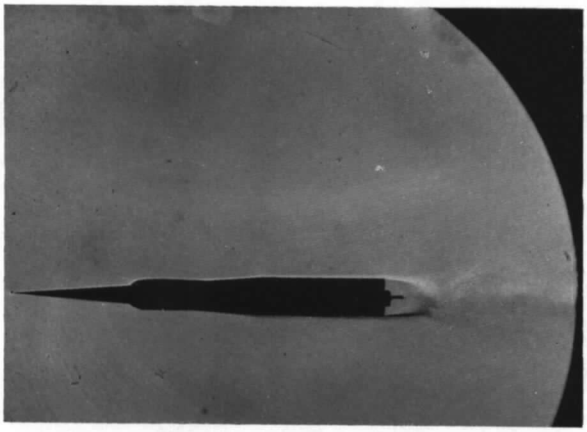

(a) $l = 0 \cdot 5h$.

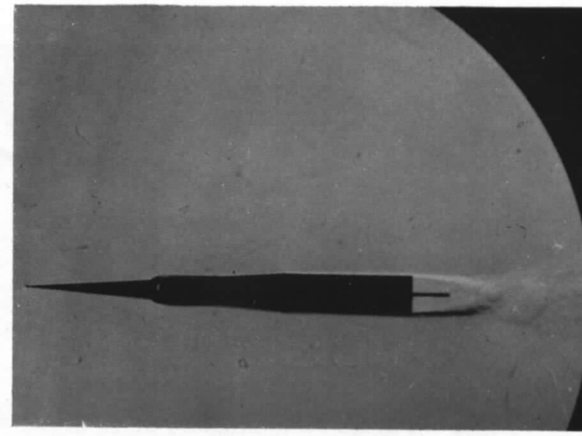

(b) $l = h$.

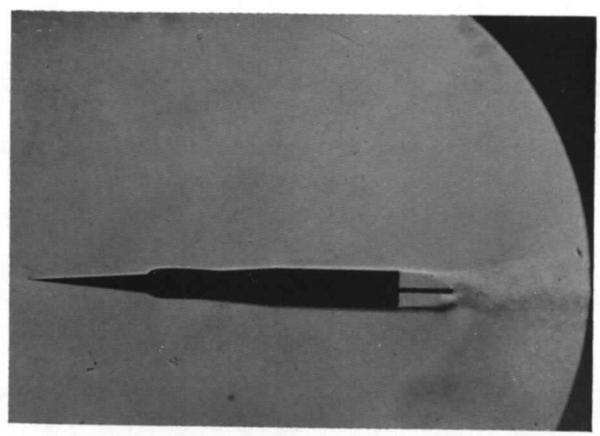

(c) $l = 1 \cdot 5h$.

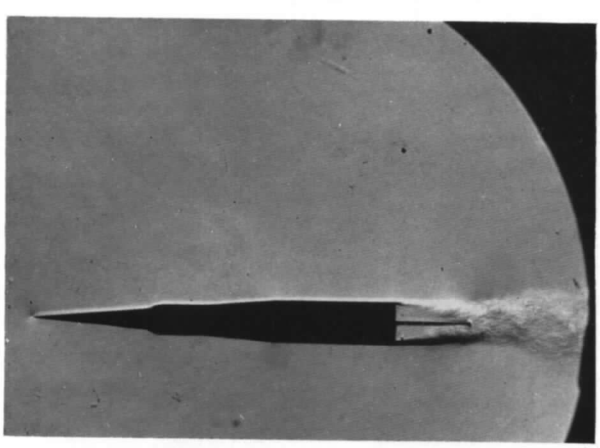

(d) $l = 2h$.

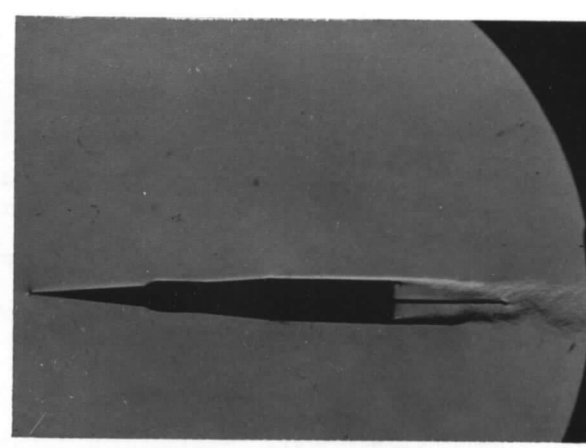

(e) $l = 3h$.

FIG. 37. The subsonic flow past the model fitted with splitter plates of various lengths. ($M_\infty = 0 \cdot 4$.)

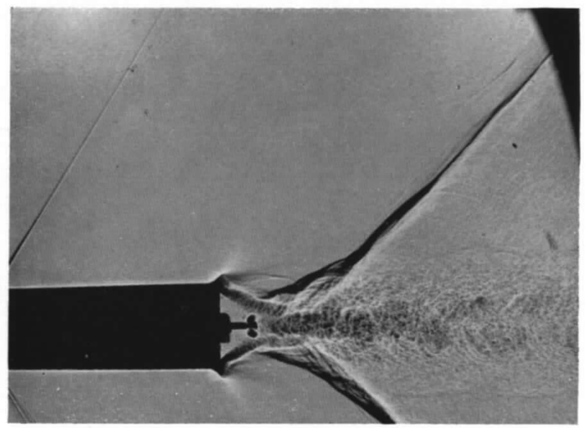

FIG. 38. Instability of the supersonic base flow in the case of the model fitted with a short splitter plate ($l = 0 \cdot 5h$). ($M_\infty = 1 \cdot 05$.) (Direct shadow photograph.)

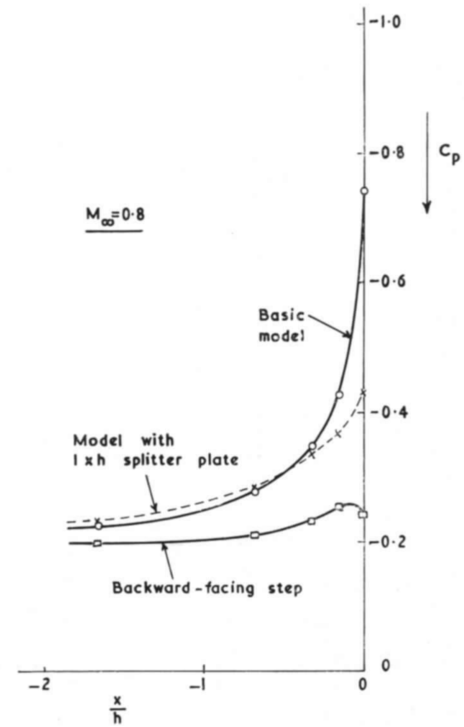

FIG. 39. Effect of base conditions on surface pressures upstream of base.

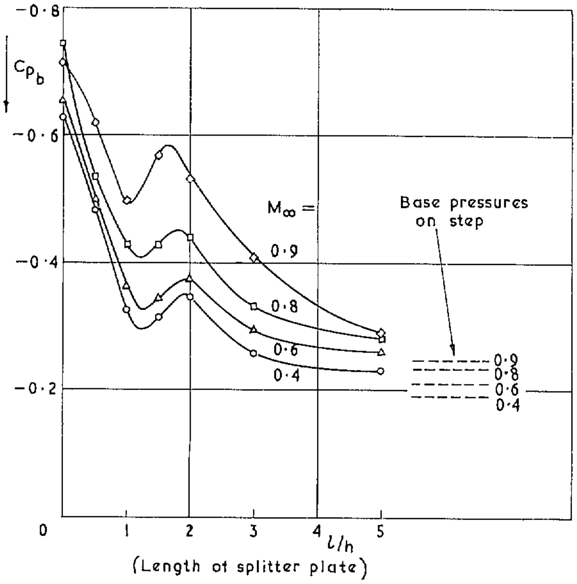

FIG. 40. Effect of splitter plate on base pressure.

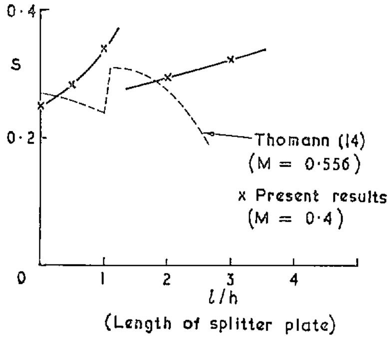

FIG. 41. Comparison of measured Strouhal numbers with results of Ref. 14.

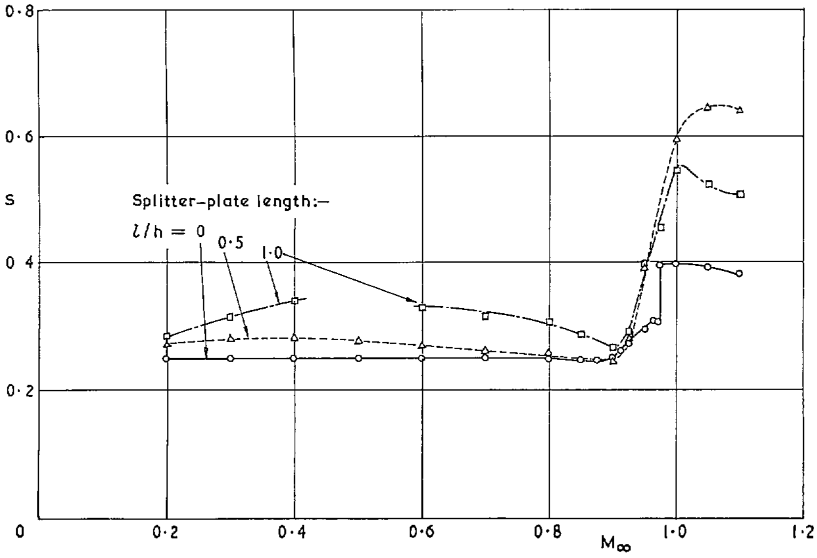

FIG. 42a. Vortex shedding frequencies for model with short splitter plates.

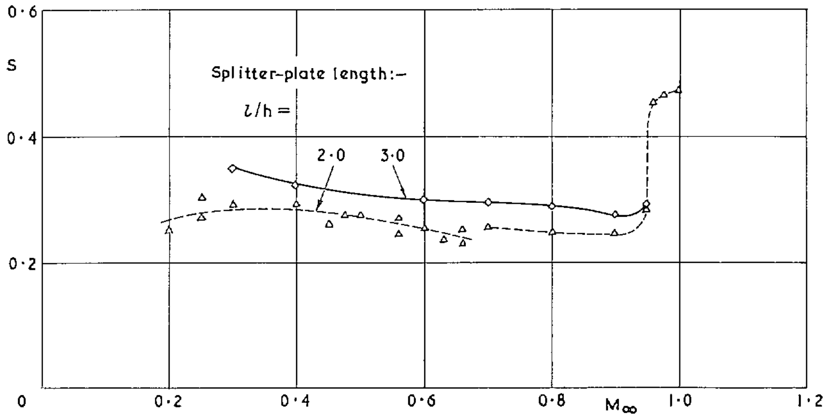

FIG. 42b. Vortex-shedding frequencies for model with long splitter plates.

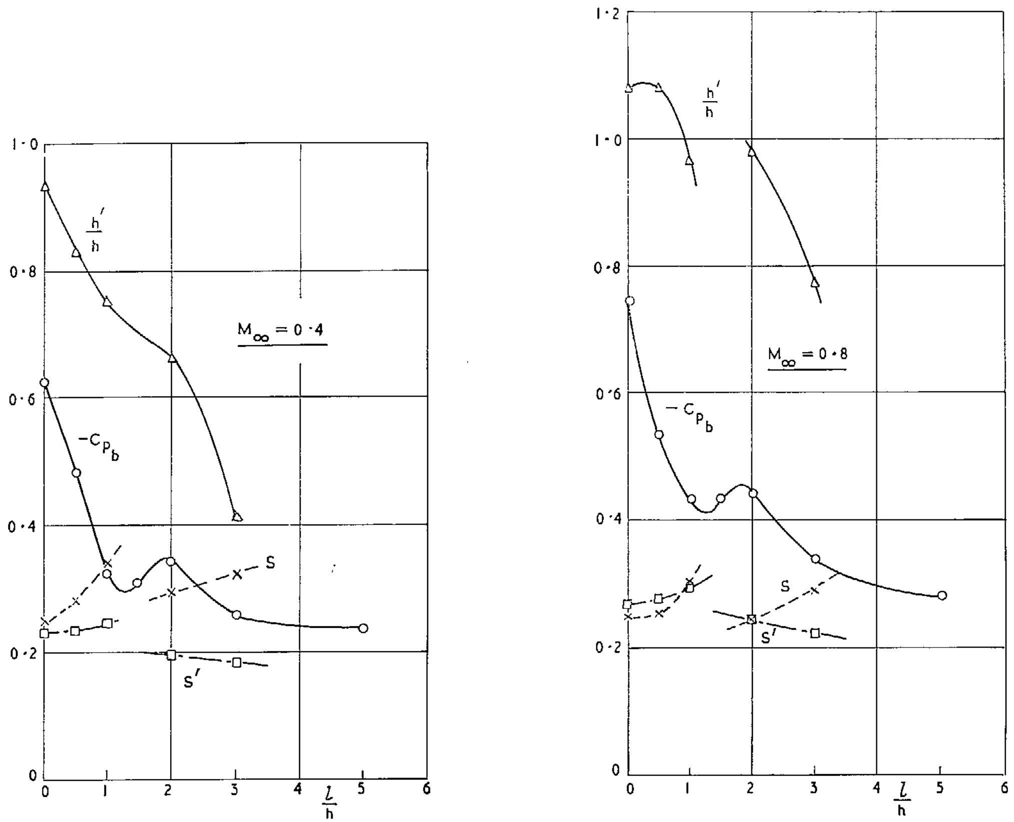

FIGS. 43a and b. Variation of Strouhal number, wake thickness and base pressure with splitter-plate length.

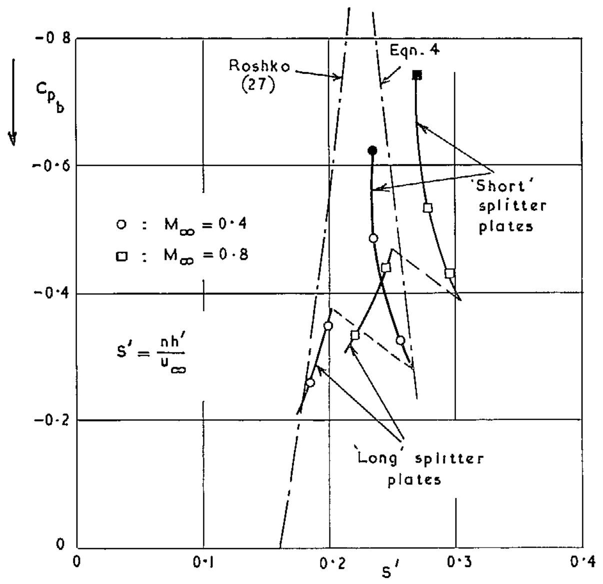

FIG. 44. Relation between Strouhal number based on wake thickness and base pressure.

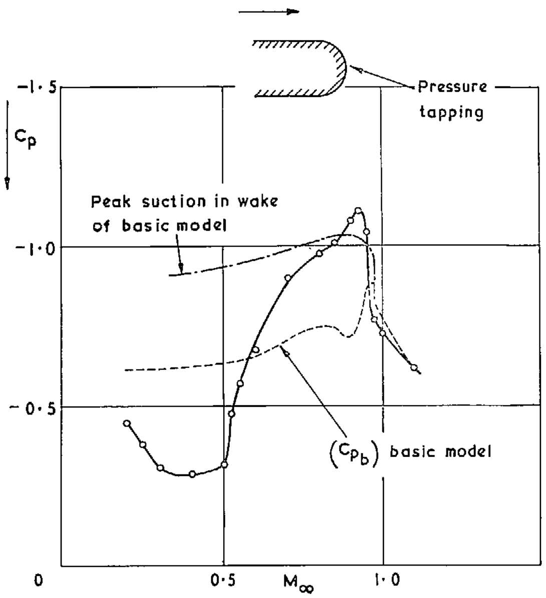

FIG. 45. Base pressure on model with half-round base.

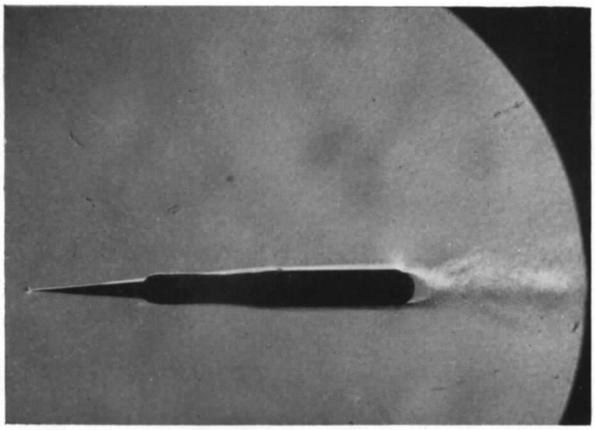

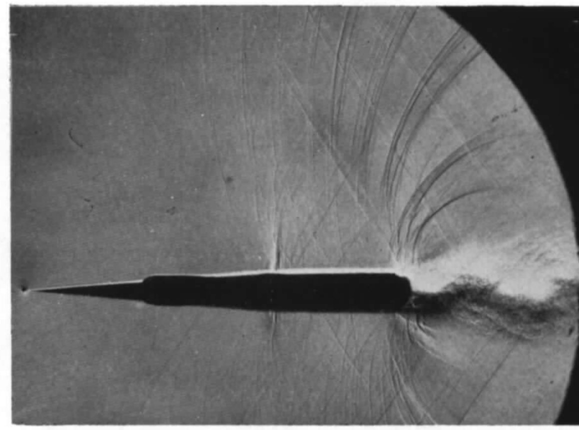

(a) $M_\infty = 0{\cdot}4$. (b) $M_\infty = 0{\cdot}8$.

FIG. 46. The rounded trailing edge.

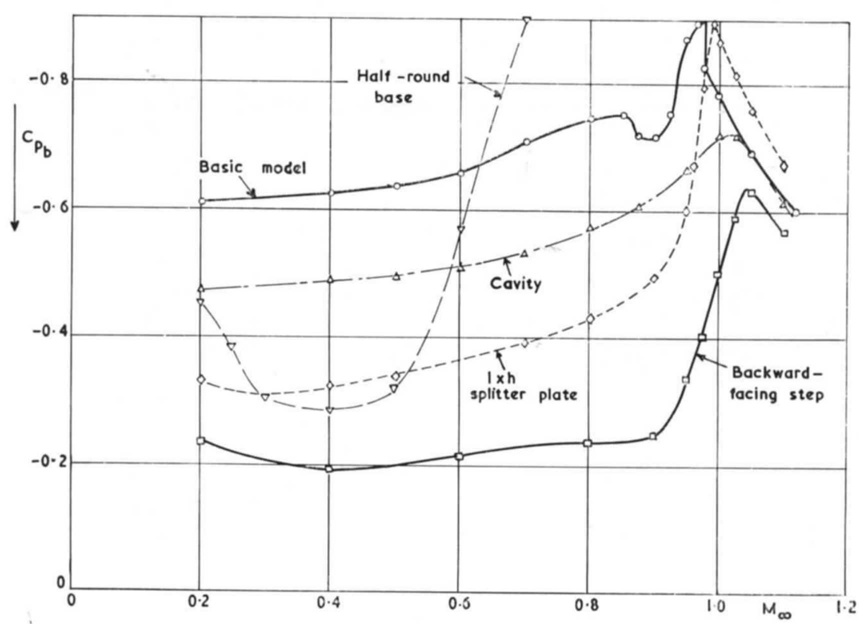

FIG. 47. Comparison of results for different base configurations. (*See* Figs. 2, 5, 6 and 7.)

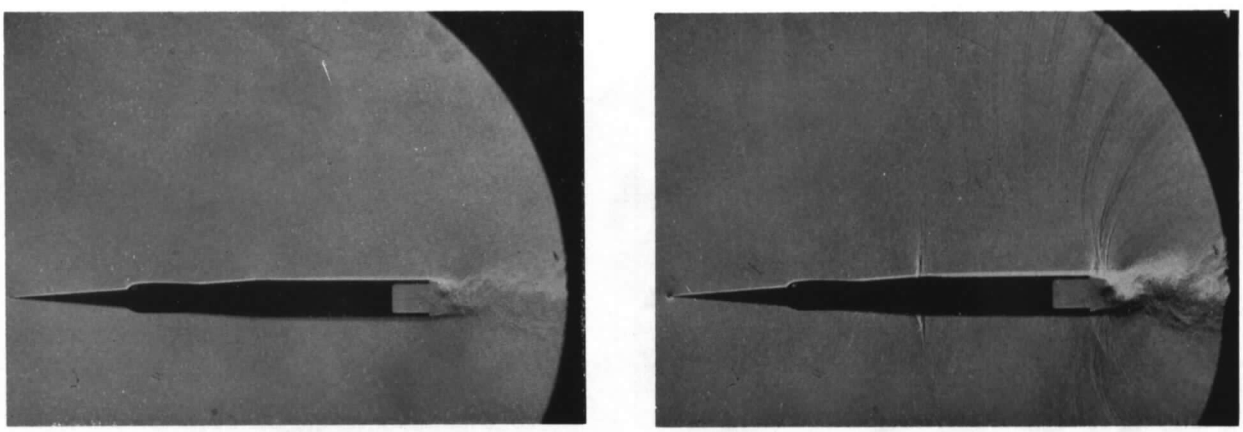

(a) $M_\infty = 0 \cdot 4$. (b) $M_\infty = 0 \cdot 8$.

FIG. 48. The trailing-edge cavity.

(92363) Wt. 67/7689 K.5 9/66 Hw.

Publications of the Aeronautical Research Council

ANNUAL TECHNICAL REPORTS OF THE AERONAUTICAL RESEARCH COUNCIL (BOUND VOLUMES)

1945 Vol. I. Aero and Hydrodynamics, Aerofoils. £6 10s. (£6 14s.)
Vol. II. Aircraft, Airscrews, Controls. £6 10s. (£6 14s.)
Vol. III. Flutter and Vibration, Instruments, Miscellaneous, Parachutes, Plates and Panels, Propulsion. £6 10s. (£6 14s.)
Vol. IV. Stability, Structures, Wind Tunnels, Wind Tunnel Technique. £6 10s. (£6 14s.)

1946 Vol. I. Accidents, Aerodynamics, Aerofoils and Hydrofoils. £8 8s. (£8 12s. 6d.)
Vol. II. Airscrews, Cabin Cooling, Chemical Hazards, Controls, Flames, Flutter, Helicopters, Instruments and Instrumentation, Interference, Jets, Miscellaneous, Parachutes. £8 8s. (£8 12s.)
Vol. III. Performance, Propulsion, Seaplanes, Stability, Structures, Wind Tunnels. £8 8s. (£8 12s.)

1947 Vol. I. Aerodynamics, Aerofoils, Aircraft. £8 8s. (£8 12s. 6d.)
Vol. II. Airscrews and Rotors, Controls, Flutter, Materials, Miscellaneous, Parachutes, Propulsion, Seaplanes, Stability, Structures, Take-off and Landing. £8 8s. (£8 12s. 6d.)

1948 Vol. I. Aerodynamics, Aerofoils, Aircraft, Airscrews, Controls, Flutter and Vibration, Helicopters, Instruments, Propulsion, Seaplane, Stability, Structures, Wind Tunnels. £6 10s. (£6 14s.)
Vol. II. Aerodynamics, Aerofoils, Aircraft, Airscrews, Controls, Flutter and Vibration, Helicopters, Instruments, Propulsion, Seaplane, Stability, Structures, Wind Tunnels. £5 10s. (£5 14s.)

1949 Vol. I. Aerodynamics, Aerofoils. £5 10s. (£5 14s.)
Vol. II. Aircraft, Controls, Flutter and Vibration, Helicopters, Instruments, Materials, Seaplanes, Structures, Wind Tunnels. £5 10s. (£5 13s. 6d.)

1950 Vol. I. Aerodynamics, Aerofoils, Aircraft. £5 12s. 6d. (£5 16s. 6d.)
Vol. II. Apparatus, Flutter and Vibration, Meteorology, Panels, Performance, Rotorcraft, Seaplanes. £4 (£4 3s. 6d.)
Vol. III. Stability and Control, Structures, Thermodynamics, Visual Aids, Wind Tunnels. £4 (£4 3s. 6d.)

1951 Vol. I. Aerodynamics, Aerofoils. £6 10s. (£6 14s.)
Vol. II. Compressors and Turbines, Flutter, Instruments, Mathematics, Ropes, Rotorcraft, Stability and Control, Structures, Wind Tunnels. £5 10s. (£5 14s.)

1952 Vol. I. Aerodynamics, Aerofoils. £8 8s. (£8 12s.)
Vol. II. Aircraft, Bodies, Compressors, Controls, Equipment, Flutter and Oscillation, Rotorcraft, Seaplanes, Structures. £5 10s. (£5 13s. 6d.)

1953 Vol. I. Aerodynamics, Aerofoils and Wings, Aircraft, Compressors and Turbines, Controls. £6 (£6 4s.)
Vol. II. Flutter and Oscillation, Gusts, Helicopters, Performance, Seaplanes, Stability, Structures, Thermodynamics, Turbulence. £5 5s. (£5 9s.)

1954 Aero and Hydrodynamics, Aerofoils, Arrester gear, Compressors and Turbines, Flutter, Materials, Performance, Rotorcraft, Stability and Control, Structures. £7 7s. (£7 11s.)

Special Volumes

Vol. I. Aero and Hydrodynamics, Aerofoils, Controls, Flutter, Kites, Parachutes, Performance, Propulsion, Stability. £6 6s. (£6 9s. 6d.)
Vol. II. Aero and Hydrodynamics, Aerofoils, Airscrews, Controls, Flutter, Materials, Miscellaneous, Parachutes, Propulsion, Stability, Structures. £7 7s. (£7 10s. 6d.)
Vol. III. Aero and Hydrodynamics, Aerofoils, Airscrews, Controls, Flutter, Kites, Miscellaneous, Parachutes, Propulsion, Seaplanes, Stability, Structures, Test Equipment. £9 9s. (£9 13s. 6d.)

Reviews of the Aeronautical Research Council

1949–54 5s. (5s. 6d.)

Index to all Reports and Memoranda published in the Annual Technical Reports

1909–1947 R. & M. 2600 (out of print)

Indexes to the Reports and Memoranda of the Aeronautical Research Council

Between Nos. 2451–2549: R. & M. No. 2550 2s. 6d. (2s. 9d.); Between Nos. 2651–2749: R. & M. No. 2750 2s. 6d. (2s. 9d.); Between Nos. 2751–2849: R. & M. No. 2850 2s. 6d. (2s. 9d.); Between Nos. 2851–2949: R. & M. No. 2950 3s. (3s. 3d.); Between Nos. 2951–3049: R. & M. No. 3050 3s. 6d. (3s. 9d.); Between Nos. 3051–3149: R. & M. No. 3150 3s. 6d. (3s. 9d.); Between Nos. 3151–3249: R. & M. No. 3250 3s. 6d. (3s. 9d.); Between Nos. 3251–3349: R. & M. No. 3350 3s. 6d. (3s. 11d.)

Prices in brackets include postage

Government publications can be purchased over the counter or by post from the Government Bookshops in London, Edinburgh, Cardiff, Belfast, Manchester, Birmingham and Bristol, or through any bookseller

R. & M. No. 3427

© *Crown Copyright 1966*

Printed and published by
HER MAJESTY'S STATIONERY OFFICE

To be purchased from
49 High Holborn, London WC1
423 Oxford Street, London W1
13A Castle Street, Edinburgh 2
109 St. Mary Street, Cardiff
Brazennose Street, Manchester 2
50 Fairfax Street, Bristol 1
35 Smallbrook, Ringway, Birmingham 5
80 Chichester Street, Belfast 1
or through any bookseller

Printed in England

R. & M. No. 3427

S.O. Code No. 23-3427